



Cite this: *Chem. Soc. Rev.*, 2023, 52, 7262

## Ionic liquids revolutionizing biomedicine: recent advances and emerging opportunities

Yanhui Hu,<sup>†abcd</sup> Yuyuan Xing,<sup>†abc</sup> Hua Yue,<sup>id†ac</sup> Tong Chen,<sup>cd</sup> Yanyan Diao,<sup>id\*abc</sup> Wei Wei,<sup>id\*ac</sup> and Suojiang Zhang<sup>id\*abc</sup>

Ionic liquids (ILs), due to their inherent structural tunability, outstanding miscibility behavior, and excellent electrochemical properties, have attracted significant research attention in the biomedical field. As the application of ILs in biomedicine is a rapidly emerging field, there is still a need for systematic analyses and summaries to further advance their development. This review presents a comprehensive survey on the utilization of ILs in the biomedical field. It specifically emphasizes the diverse structures and properties of ILs with their relevance in various biomedical applications. Subsequently, we summarize the mechanisms of ILs as potential drug candidates, exploring their effects on various organisms ranging from cell membranes to organelles, proteins, and nucleic acids. Furthermore, the application of ILs as extractants and catalysts in pharmaceutical engineering is introduced. In addition, we thoroughly review and analyze the applications of ILs in disease diagnosis and delivery systems. By offering an extensive analysis of recent research, our objective is to inspire new ideas and pathways for the design of innovative biomedical technologies based on ILs.

Received 2nd July 2023

DOI: 10.1039/d3cs00510k

[rsc.li/chem-soc-rev](https://rsc.li/chem-soc-rev)

<sup>a</sup> Beijing Key Laboratory of Ionic Liquids Clean Process, CAS Key Laboratory of Green Process and Engineering, State Key Laboratory of Multiphase Complex Systems, State Key Laboratory of Biochemical Engineering, Institute of Process Engineering, Chinese Academy of Sciences, Beijing 100190, China.  
 E-mail: [yydiao@ipe.ac.cn](mailto:yydiao@ipe.ac.cn), [weiwei@ipe.ac.cn](mailto:weiwei@ipe.ac.cn), [sjzhang@ipe.ac.cn](mailto:sjzhang@ipe.ac.cn)

<sup>b</sup> Innovation Academy for Green Manufacture, Chinese Academy of Sciences, Beijing 100190, China

<sup>c</sup> College of Chemical and Engineering, University of Chinese Academy of Sciences, Beijing 100049, China

<sup>d</sup> Chengdu Institute of Organic Chemistry, Chinese Academy of Sciences, Chengdu 610041, China

<sup>†</sup> These authors contributed equally: Yanhui Hu, YuYuan Xing, Hua Yue.

## 1 Introduction

Ionic liquids (ILs) are a class of molten salts, exhibiting a vast diversity with nearly  $10^{18}$  potential combinations.<sup>1</sup> ILs have a history of more than 100 years, starting with the synthesis of liquid ethylammonium by Walden in 1914.<sup>2</sup> However, the first-generation ILs were unstable and sensitive to water and air, which limited their applications. The second-generation ILs emerged in 1992 with the synthesis of a stable 1-ethyl-3-methylimidazolium cation IL,<sup>3</sup> in which the anions were replaced by weak coordination anions such as tetrafluoroborate and hexafluorophosphate ([BF<sub>4</sub>] and [PF<sub>6</sub>]). From then on, the



**Yanhui Hu**

Yanhui Hu is a PhD candidate at Chengdu Institute of Organic Chemistry, Chinese Academy of Sciences (CAS), majoring in applied chemistry. At present, she is studying at Beijing Key Laboratory of Ionic Liquids Clean Process, Institute of Process Engineering (IPE). Her current research interests focus on ionic liquids' toxicity on organisms and the new applications of ionic liquids in biomedicine.



**Yuyuan Xing**

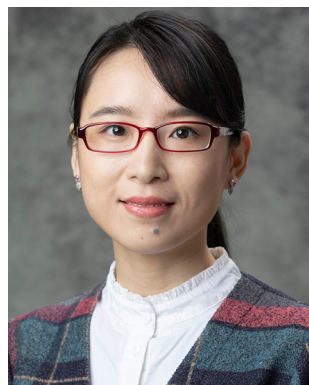
Yuyuan Xing is a PhD candidate at the IPE, CAS. She is majoring in Chemical Engineering at Beijing Key Laboratory of Ionic Liquid Cleaning Process, IPE. Her current research focuses on biotoxicology of ionic liquids.



research of ILs has progressed rapidly. After 2000, ILs can be functionally designed according to their physicochemical properties; so ILs have rapidly entered into the third-generation.<sup>4</sup> Compared with the previous two generations, the third-generation ILs have been developing quickly. They are biodegradable and biocompatible (such as natural alkalis like choline, amino acids, and carboxylic acids). Throughout the development history of ILs, from unstable to stable states, and then to the designability of structures, ILs have gradually played an important role in many fields such as chemistry, energy, and machinery.

As early as 2001, ILs were researched as antibacterial agents.<sup>5</sup> Since then, the third-generation ILs have gradually been explored in multiple fields of biomedicine. ILs' diverse ranges of structures allow for the customization of their physicochemical properties, making ILs highly advantageous in pharmaceutical applications. Specifically, ILs demonstrate

potential in the development of drugs with antibacterial and anticancer properties by virtue of their ability to disrupt pathogen cell membranes and organelles.<sup>6,7</sup> Another notable advantage is their miscibility, which can significantly improve the solubility of drugs and enhance the bioavailability of poorly soluble drugs. Furthermore, the tunability of ILs allows for the customization of their properties, including acidity, alkalinity, and H-bonds, which makes ILs highly versatile in pharmaceutical engineering, particularly as drug extractants and catalysts. Moreover, the modular nature of ILs enables the design of targeted drugs with responsive release capabilities. By tailoring the properties of ILs, drugs can be precisely released on-demand, enhancing their therapeutic efficacy. ILs can also form clusters, allowing for efficient loading and delivery of drugs, which can encapsulate drug molecules, protect drugs from degradation, and facilitate their controlled release at the desired site of action. Additionally, the high conductivity of ILs



**Hua Yue**

*Hua Yue is an associated professor in IPE, CAS. She received her BS degree (2008) from Shandong University and PhD degree (2012) from IPE, CAS. Her research is focused on exploring novel micro/nano materials for tumor therapy or vaccine delivery. She has published 55 papers on academic journals (e.g., Nature Communications, Science Advances, and Advanced Drug Delivery Reviews), and 3 edited book chapters and has*

*been granted 4 patents. Her work on the biological effects of nanomaterials has been evaluated as "one of the most systematic studies".*



**Yanyan Diao**

*Yanyan Diao received her PhD from CAS Key Laboratory of Green Process and Engineering, IPE, CAS, in 2009 and then stayed there to work as an assistant professor. In 2012, She was promoted to an associate professor. Her research is focused on the properties of ionic liquids and the applications of ionic liquids in green process engineering. She has won the second prize of Technology Progress of China Petroleum and Chemical Association.*



**Wei Wei**

*Wei Wei received his PhD from the State Key Laboratory of Biochemical Engineering, IPE, CAS, in 2011. In 2013, he was promoted to an associate professor and became a full professor in 2018. He was also supported by the National Science Fund for Distinguished Young Scholars because of his outstanding achievements. His current research focuses on biomimetic formulation engineering for anticancer therapy. He has published over 130 papers in*

*influential academic journals (e.g., Nature Nanotechnology, Nature Biomedical Engineering, and Science Translational Medicine).*



**Suojiang Zhang**

*Prof. Suojiang Zhang is currently the Director General of IPE, CAS, Dean of College of Chemical Engineering, University of Chinese Academy of Sciences (UCAS), and a Fellow of Royal Society of Chemistry (RSC). He was elected as a Member of CAS in 2015. Prof. Zhang's research interests focus on green chemistry and process engineering. He is dedicated to promoting innovation and application of ionic liquids in green process engineering and*

*has achieved groundbreaking results. He has published over 600 peer-reviewed articles, authored 11 monographs and has been granted more than 290 patents.*







structures. In terms of cations, they are organic in nature and can be classified into imidazole, pyridine, piperidine, amine, pyrrole, morpholine, and phosphine. For anions, they can be organic (amino acid salt, benzene sulfonate, *etc.*) or inorganic (halide, tetrafluoroborate, hexafluorophosphate, *etc.*). Functional groups, such as cyano, hydroxyl, ether, amino, sulfonic, ester, and carboxyl, introduced into the structure can realize functionalized ILs with different properties.<sup>17–20</sup> In general, the selection of anions and substituents can affect the acidity and alkalinity of ILs.

A full understanding of the microstructures of ILs provides a research basis for the cognizance of the properties and possible applications. The diverse structures of ILs provide the ability to control the quantitative structure–activity relationship in terms of biological and chemical properties by precise changes in chemical structures, thereby increasing the range of applications and trials in the pharmaceutical industry. For example, the design and synthesis of targeted groups with pH (*e.g.*, imine bond, carboxyl group), optical (*e.g.*, azobenzene and cinnamic acid group), and magnetic (*e.g.*, combined with magnetic nano) responses are based on the characteristics of ILs with many kinds and strong designability. By selecting the appropriate combination of cations and anions, scientists can construct different biomedical ILs.

## 2.2 Interaction forces in ILs

The unique properties of ILs are closely related to their structure and the interactions between ions. The structural parameters of ILs also have a significant impact on drug loading and release behavior.<sup>21</sup> The properties of ILs are governed by various forces, including Coulombic, dispersion, H-bonding forces, van der Waals interactions (dipole-induced dipole, dispersion), and possible  $\pi$ – $\pi$  or  $n$ – $\pi$  stacking, which can be adjusted by changing the type of cation or anion and the length or the number of attached organic chains.<sup>22,23</sup> H-bonds, which are electrostatic attractions between protons in one molecule and negatively charged atoms in another, are crucial for the structure and interaction modes of ILs.<sup>24</sup>

H-bonds play a crucial role in the stability and miscibility of miscible systems,<sup>25,26</sup> as well as determining the hydrophilic and hydrophobic properties of ILs.<sup>27</sup> In general, ILs interact with water primarily through the anions in the aqueous solution.<sup>28</sup> For example, the strength of H-bonds between water and anions follows the order  $[\text{PF}_6]^- < [\text{SbF}_6]^- < [\text{BF}_4]^- < [(\text{CF}_3\text{SO}_2)_2\text{N}]^- < [\text{ClO}_4]^- < [\text{CF}_3\text{SO}_3]^- < [\text{NO}_3]^- < [\text{CF}_3\text{CO}_2]^-$ .<sup>29</sup> The existence of a small amount of water would also have a great impact on the H-bonding network of ILs.<sup>30</sup> Water and ILs' anions form new H-bonds, which could destroy the H-bond interaction between ion pairs in the original ILs. It should be noted that the cations of ILs also have a significant influence on the hydrophilicity and hydrophobicity of ILs.<sup>31</sup> Given that hydrophilicity is a critical factor in the application of ILs in water-based systems and that water is the predominant substance in physiological environments, modular and interactive methods can be used to design ILs by understanding and predicting the impact of H-bonds. Specifically, the disadvantages of given anions with low water

solubility can be mitigated by changing the counter cation with the ability to strengthen the H-bonds with water.<sup>31</sup>

H-bonding networks can be present in pure ILs. The strong interactions between anions and cations, as well as the large molecular volume and H-bond directions, allow ILs to self-assemble into various heterogeneous structures in a medium, such as vesicles, micelles, and microemulsions (Fig. 2A).<sup>32</sup> These IL clusters are crucial for interpreting many physical phenomena of ILs, such as heterogeneous self-diffusion, surface layering, and surfactant-like micelles formed in IL–water mixtures.<sup>33</sup> Vesicles are membrane-like self-assembled hollow structures formed by amphiphilic substances in solvents.<sup>34</sup> Wang *et al.* first observed that 1-alkyl-3-methylimidazolium bromides  $[\text{C}_n\text{MIM}][\text{Br}]$  ( $n = 10, 12, \text{ and } 14$ ) could be self-assembled to unilamellar vesicles in aqueous solutions without any additives.<sup>35</sup> In this study, it was found that the clusters formed by ILs in water were larger than 200 nm. Micelles are amphiphilic structures, typically consisting of a hydrophilic periphery and a hydrophobic core, which can be used for encapsulating hydrophobic drugs. Goto *et al.* synthesized IL-based micelles, which incorporated a large number of drugs into the hydrophobic core through H-bonding interactions between ILs and the drug molecules.<sup>36</sup> Microemulsion is usually defined as a stable, isotropic mixed solution composed of water, oil, a cosurfactant, and a surfactant, with three types: oil-in-water, water-in-oil, and bicontinuous.<sup>37,38</sup> For example, the encapsulation of rifampicin was achieved through the use of a microemulsion system, which comprised the hydrophobic IL 1-butyl-3-methylimidazolium hexafluorophosphate ( $[\text{BMIM}][\text{PF}_6]$ ), along with non-ionic surfactants (Brij35, TX100) and water. In this system,  $[\text{BMIM}][\text{PF}_6]$  acted as the oil phase. The rifampicin was loaded into the microemulsion near the palisade layer/apolar side or towards the core of the microstructures.<sup>39</sup> This method offers an enhanced approach for drug loading, stability, and controlled release properties.

The types of clusters formed by ILs could be transformed under different conditions (Fig. 2B). For instance, the vesicular and micellar structure of ILs could be altered by adjusting the pH.<sup>40</sup> In another example, reversible transformations between micelles and vesicles of ILs (4-butylazobenzene-4'-hexyloxytrimethyl-ammoniumtrifluoro-acetate) were achieved through UV and visible-light irradiation, which could be exploited for light-responsive drug delivery.<sup>41</sup> Similarly, 1-tetradecyl-3-methylimidazolium 1,2,3-benzotriazole ( $[\text{C}_{14}\text{MIM}][1, 2, 3\text{-Ben}]$ ) exhibited a reversible conversion structure from vesicles to micelles in the presence of alternating  $\text{CO}_2$  and  $\text{N}_2$  bubbling.<sup>42</sup> Chandrakar and Bhargava investigated the aggregation of a hydroxy functionalized IL (1-(*n*-hydroxyalkyl)-3-(*n*-hydroxyalkyl) imidazolium bromide ( $[\text{HOC}_n\text{C}_m\text{OHI}_m][\text{Br}]$ ) ( $n = 2, 6, 10, \text{ or } 14$ ) in aqueous solutions using atomistic molecular dynamics (MD) simulations.<sup>45</sup> They found that the length of the hydroxyalkyl chains played a key role in determining the structures of the formed clusters. Specifically, the length of the substituent determined the ILs' morphology. Small clusters could be formed when one of the substituents was a hydroxydecyl chain. However, when the substituent was hydroxyldodecyl or hydroxyl



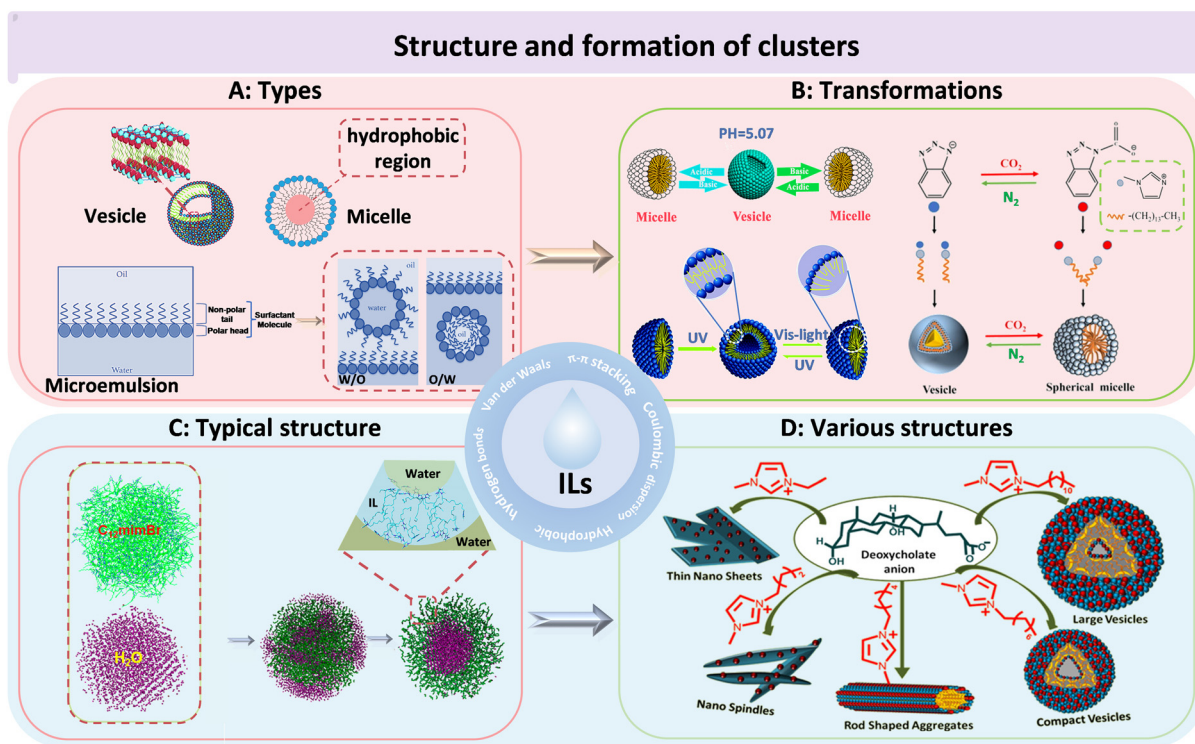


**Fig. 2** The structures and morphologies of ILs. (A) The categories of IL-based clusters. Vesicle (left), micelle (right), microemulsion (bottom). Reproduced with permission from ref. 34 and 38. Copyright 2015 Royal Society of Chemistry and 2017 Elsevier. (B) The transformations of IL clusters under different environmental conditions. pH-induced reversible transition of  $[C_{14}MIM][H_4COOKCOO]$  clusters in aqueous solution (left). UV/light-induced reversible transition of 4-butylazobenzene-4'-hexyloxytrimethyl-ammoniumtrifluoro-acetate clusters in aqueous solution (bottom).  $[C_{14}MIM][1,2,3-Ben]$  cluster transition by bubbling  $CO_2$  (right). Reproduced with permission from ref. 40–42. Copyright 2014 American Chemical Society, 2015 Royal Society of Chemistry and 2022 Elsevier. (C) The clusters of  $[C_{12}MIM][Br]$  in water. Green:  $[C_{12}MIM]^+$ , magenta:  $H_2O$ .<sup>43</sup> Reproduced with permission from ref. 43. Copyright 2015 American Chemical Society. (D) The cluster structure of  $[C_nmim][DC]$  changed with the length of the carbon chain.<sup>44</sup> Reproduced with permission from ref. 44. Copyright 2018 American Chemical Society.

tetradecyl chains, the solution structure was arranged as a thin film. Additionally, the concentration of ILs affected the types of clusters, with spherical micelles transitioning to rod-like micelles and then to vesicles with increasing concentration<sup>35</sup> The morphology of ILs in water was typically spherical, with imidazole rings being mainly located near the interface between vesicles and water and dodecyl groups buried in two layers composed of imidazole rings (Fig. 2C).<sup>43</sup> Besides being spherical, IL clusters can also take on other shapes, such as thin nanosheets, nanospindles, and rod shaped clusters (Fig. 2D).<sup>44</sup> In addition to the diversity of morphology, for size, simulations and TEM studies have revealed that IL clusters, which were primarily focused on IL complexes could range in size from a few nanometers to several hundred nanometers.<sup>36,37,39,44</sup>

Currently, research on IL clusters has been widespread, focusing on their formation principles and compositional structures. IL clusters are highly influenced by cationic side chain lengths and anion types, which can lead to a diverse range of possible spatially organized structures. For example, Wang and Voth explored the effect of various cationic side chain lengths on ILs by a multiscale coarse graining. The simulation results showed that neutral tail groups of cations aggregated to form spatially heterogeneous domains of the tails with sufficient side chain length, while the charged head

groups and anions distributed homogeneously due to the strong electrostatic interactions.<sup>46</sup> Wang's team discovered that the hydrophobicity and aromaticity of IL anions played a crucial role in the formation of clusters. The influence of anions on the formation of IL clusters was attributed to the synergistic effect of hydrophobic and  $\pi$ - $\pi$  interactions.<sup>42</sup>

A comprehensive understanding of the self-assembly mechanism of ILs can provide valuable theoretical guidance and assistance for designing IL clusters with various sizes, types, shapes, and properties for different applications. In particular, when combined with biomedical research, such as the mechanism of drug delivery and interaction with various organisms, ILs' aggregations hold great potential and merit further attention and in-depth investigation. Notably, the occurrence of experimental phenomena cannot be fully explained when ILs are completely composed of ions in the industrial field.<sup>2</sup> Currently, molecular simulation is the primary method of predicting the formation process and structural characteristics of IL clusters. The behavior and morphology of IL clusters as biological carriers need to be further validated by experiments to fully uncover the true IL cluster characteristics. In addition, despite significant progress in the use of ILs in biomedicine, their underlying mechanisms remain unclear. Many structural factors related to ILs require investigation, *e.g.*, their states *in vivo* and *in vitro*,



their impacts on cells, and whether cluster formations affect metabolic processes *in vivo*.

### 2.3 Physicochemical properties of ILs

In addition to the IL cluster structure, other inherent properties of ILs, such as the melting point, electrochemical characteristics, and solubility, are closely related to their wide range of applications in various fields. ILs usually have a melting point below 100 °C and are liquid at room temperature, making them beneficial for use in medicine at physiological temperatures. The main reason for the low melting point of ILs is that the ion asymmetry forms a loose structure, which cannot be closely stacked. The melting point of ILs is also related to ionic size, delocalization of charge, and H-bonds.<sup>47–49</sup> Deep eutectic solvents (DESs) are mixtures based on ILs that have a lower melting point than any of their individual components (*e.g.*, choline chloride and urea).<sup>50</sup> Generally, DESs can alter the physicochemical properties of ILs, such as the melting point, density, viscosity, and surface tension.<sup>51</sup> Third-generation ILs and DESs have been gradually developed with continuously improved formulae in the fields of drug synthesis and drug delivery because of their liquidity at room temperature and good biocompatibility.

ILs possess excellent conductivity, due to the wide electrochemical potential window and medium conductivity, typically between 10 and 20 mS cm<sup>-1</sup>.<sup>52</sup> And, their liquid state allows for the free movement of anions and cations, which contributes to their inherent conductivity. The wide electrochemical potential window represents the stable electrochemical properties and mainly depends on the reduction resistance of cations and the oxidation resistance of anions.<sup>53</sup> Conductivity is a measured value indicating the ability of a material to transmit electrons. Generally, high conductivity is accompanied by high liquid density, low viscosity, small ionic size, high mobility, *etc.*<sup>4,54</sup> These factors are usually related to both external (environment) and internal (the structure of ILs) factors. For example, the viscosity of ILs is positively correlated with temperature. Thus, temperature is also a factor to be considered for conductivity. For internal factors, the types of cation and anion can affect the conductivity of ILs.<sup>55–57</sup> The wide electrochemical window and superior electrochemical performance of ILs lead to their application in diagnostic medicine, such as using as an electrolyte and a modified electrode in the production and improvement of the performance of sensors.

Solubility is a crucial property to be considered in the process of drug development because it can directly affect the bioavailability of drugs *in vivo*. Inorganic and organic compounds have shown remarkable solubility in various ILs. The primary distinguishing characteristic between ILs and traditional organic solvents is solvent miscibility behavior, particularly with water. Generally, ILs that contain hydrophilic groups like hydroxyl or carboxyl groups can form a uniform mixed phase with water; while ILs with highly fluorinated and charged delocalized anions, such as bis(trifluoromethanesulfonyl)imide ([NTf<sub>2</sub>]) and [PF<sub>6</sub>] undergo liquid/liquid two-phase separation with water.<sup>58</sup> This behavior can be attributed to the weak

interaction between ILs and water.<sup>59</sup> Moreover, the hydrophilicity of ILs continues to decrease with the length of the cation alkyl chain.<sup>60</sup> The hydrophilicity and hydrophobicity of ILs can be regulated by adjusting anions, cations and substituents. For example, the hydrophobicity of [NTf<sub>2</sub>] can be mitigated by incorporating compensating cationic hydrophilic groups that enhance the IL's ability to accept and donate H-bonds to water.<sup>59</sup> Therefore, most ILs have amphiphilic properties serving as a bridge between water and insoluble drugs and providing excellent solubility for many active pharmaceutical ingredients.

As neoteric solvents, ILs offer the potential to predict, adjust, and design properties, such as polarity, hydrophobicity, and solvent compatibility by imparting the different substituents, cations, and anions.<sup>61</sup> Biocompatible ILs are often derived from natural or human metabolites, such as choline and phospholipid derivatives as cations and long-chain fatty acids, amino acids, and carboxylic acids as anions.<sup>61–64</sup> In contrast, some research on toxicity of ILs suggests that it is possible for them to be used as active drug ingredients.<sup>65</sup> Given the advantages of ILs, such as a low melting point, morphological diversity, and excellent miscibility, we should expand our horizons and make use of their toxicity and biocompatibility in biomedical applications.

## 3 Therapeutic components and mechanism

### 3.1 ILs as drug candidates

ILs have shown potential in the treatment of various diseases, including bacterial and fungal infections, inflammation, cancer, and other illnesses. The wide range of possible cation and anion combinations in ILs allows for the design of molecules with inherent resistance to specific diseases. Additionally, existing drugs can be modified into ILs to improve their therapeutic properties, such as solubility and absorption rates. In this section, we will discuss and summarize the application potential of ILs in antibacterial, antifungal, anti-inflammatory, anticancer and other diseases in recent years. Fig. 3 shows some examples of the application of ILs as drug candidates including as antibacterial, antifungal, anti-inflammatory, anti-cancer, and anti-oxidative agents.

**3.1.1 ILs as antibacterial agents.** It is crucial to explore alternative antibacterial agents because of the misuse and overuse of antibiotics that have led to the development of bacterial resistance to antibacterial agents. ILs offer a promising strategy to address this issue.<sup>79</sup> Due to the negative electrostatic charge present on bacterial cell surfaces,<sup>80,81</sup> the cations of ILs can easily affect the bacterial surface.<sup>82,83</sup> Meanwhile, the combination of different cations and anions produces a wide range of ILs with tunable structures, enabling the customization of their properties against bacteria, such as Gram-positive *Staphylococcus aureus* (*S. aureus*), Gram-negative *Pseudomonas aeruginosa* (*P. aeruginosa*), and *Escherichia coli* (*E. coli*). The tunability of ILs makes it possible for them to meet different antibacterial demands. This section provides a detailed description





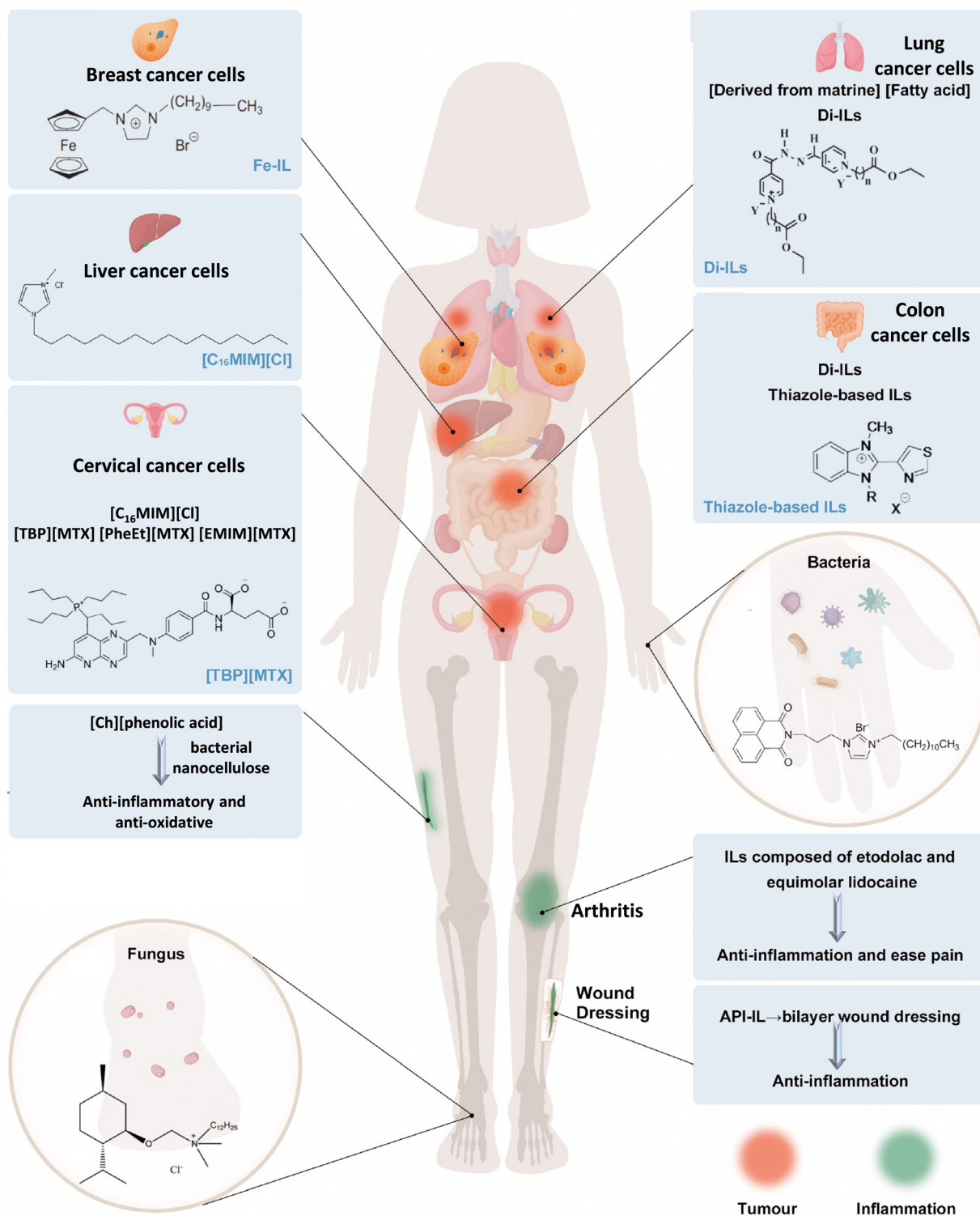


**Fig. 3** Schematic diagram of ILs as drug candidates including as antibacterial, antifungal, anti-inflammatory, anticancer, and anti-oxidative. The top human body represents the application exploration of ILs as anticancer agents.<sup>65–73</sup> The bottom human body represents the application exploration of ILs as antibacterial, antifungal, anti-inflammatory, and anti-oxidative.<sup>74–78</sup> The IL application in this picture does not represent *in vivo* experiments.

of the relationship between the ILs' structure and antibacterial activity.

Cations with an increasing number of alkyl side chains exhibit significant antimicrobial activity.<sup>84</sup> This phenomenon,



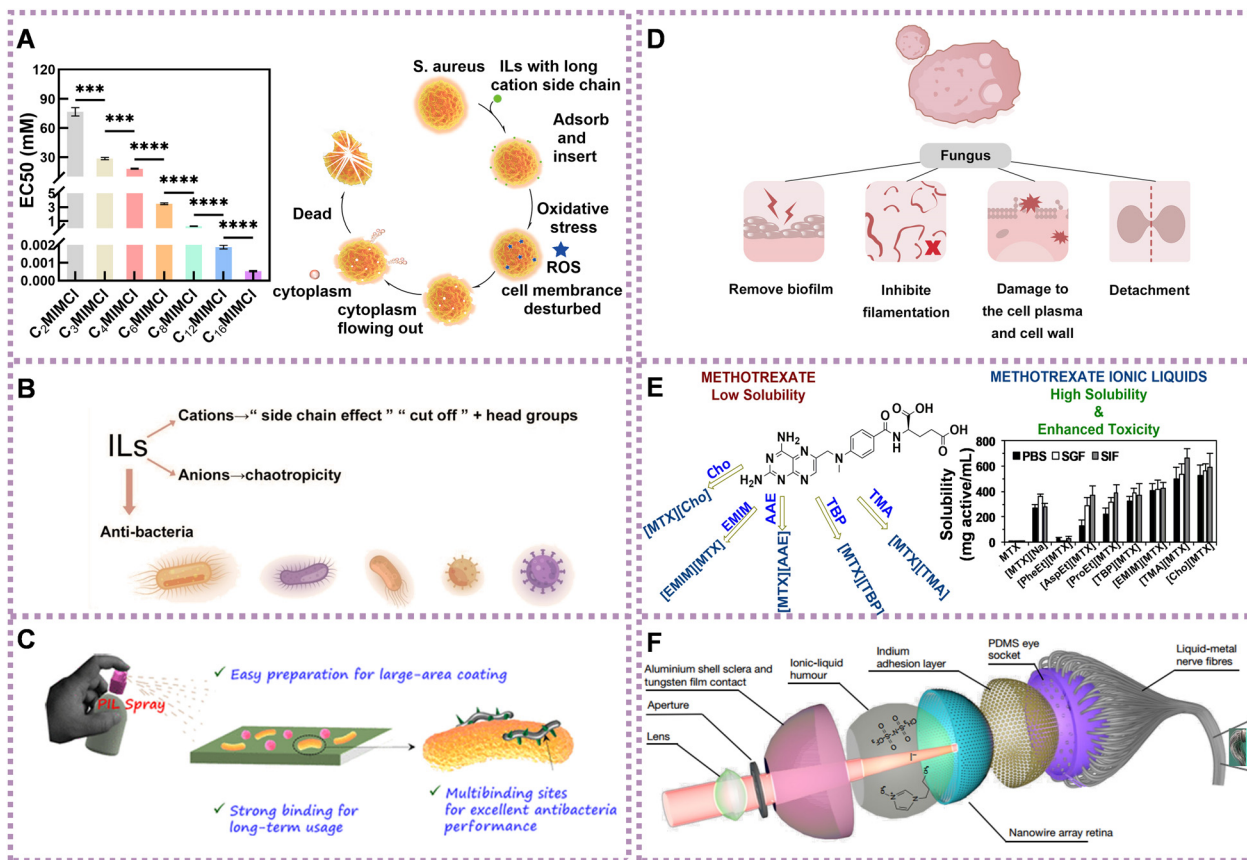


Fig. 4 Application of ILs in the treatment of diseases. (A) The toxicity of ILs to *S. aureus* increasing with cation side chain (left) and the antibacterial mechanism of ILs with long cation side chain against *S. aureus* (right). Reproduced with permission from ref. 82. Copyright 2023 by the authors, licensee Frontiers Media S.A. (B) Summary diagram of antibacterial activity of ILs. (C) Schematic diagram of universal PIL-based antiseptic spray. Reproduced with permission from ref. 91. Copyright 2021 American Chemical Society. (D) Summary of the antifungal mechanism of ILs. (E) Structure (left) and anticancer activity of several ILs (right). Reproduced with permission from ref. 70. Copyright 2019 Elsevier. (F) Detailed structure of spherical biomimetic electrochemical eye. Reproduced with permission from ref. 92. Copyright 2020 Springer Nature.

known as the 'side-chain effect,' refers to the heightened toxicity observed in longer alkyl side chains due to their increased lipophilicity.<sup>74,84–87</sup> This higher lipophilicity contributes to the enhanced antimicrobial properties of the ILs. Recently, we found that the antibacterial activity of ILs increased with the increase of the cation side chain. Driven by hydrophobicity, the long cation side chain of ILs could penetrate the cell membrane of *S. aureus* and cause complete disruption (Fig. 4A).<sup>82</sup> Chao *et al.* demonstrated that ILs with longer alkyl chains exhibited enhanced antibacterial effects against *S. aureus* and *E. coli*. These effects were attributed to the interplay of hydrophobic and electrostatic interactions between the ILs and bacterial membranes.<sup>83</sup> However, there is a cut-off point beyond which the toxicity does not indefinitely increase.<sup>88</sup> This phenomenon may be caused by the insufficient solubility of ILs, a decrease in perturbation, kinetic aspects, or an increase in spatial hindrance.<sup>89,90</sup>

Moreover, the antibacterial effect of ILs can be tuned by changing the type of cation, or modifying the cation head group. When the alkyl chain length was fixed to 12, the antibacterial activities of the following cations decreased in

the order: 1-methyl-imidazolium > piperidinium > pyrrolidinium > morpholinium for *S. aureus*, *S. epidermidis*, *E. coli*, and *E. faecalis*. When substituents such as alcohol, glucose, ether and terpene were introduced, the antibacterial activity of ILs decreased.<sup>93</sup> When the tris(pentafluoroethyl)trifluorophosphate anion ILs encountered hydrophobic or bulky cations, they could form a highly correlated ion pair, leading to a significant reduction in ion-mediated toxicity. A possible explanation was that the ion pair was no longer permeable into the bacterial membrane.<sup>85</sup>

Compared with the cationic ILs, the influence of the anionic ILs has been less investigated. However, the antibacterial behavior of anions has been an important factor, especially for ILs with less toxic cations.<sup>94–96</sup> When paired with chaotropic anions, ILs with cations exhibit enhanced antibacterial activity compared to ILs with non-chaotropic anions. The stronger chaotropic anions promote destabilization and disruption of bacterial cell membranes, increasing the susceptibility of bacteria to the ILs' antimicrobial effects.<sup>97</sup> Based on the above, the antibacterial mechanism of ILs could be modulated and controlled through the mediation of side chains, head groups, and chaotropy (Fig. 4B).





In addition, monomers with antimicrobial properties are often synthesized into IL polymers (PILs) with antibacterial effects. These PILs can be fabricated into various formulations, such as membranes and sprays, with unique advantages, such as long-term stability and effectiveness or ease of carrying, to fulfill different roles in different situations. Zhang *et al.* developed PIL-based microneedle (PIL-MN) patches loaded with salicylic acid to treat acne infections. The PIL-MN patches were synthesized by linking the 3-heptyl-1-vinylimidazolium IL, which exhibited high antimicrobial activity against Gram-positive *S. aureus*, *Propionibacterium acnes*, as well as Gram-negative *E. coli*.<sup>98</sup> He *et al.* constructed a PIL brush-grafted biomimetic sharklet surface to prevent biofouling. The PIL brushes demonstrated good antibacterial properties against both *S. aureus* and *E. coli* and anti-bovine serum protein adhesion activity, resulting from the synergistic effect of the cationic imidazole and benzotriazole groups.<sup>99</sup> Guo *et al.* found that tryptophan ions showed a synergistic effect with cations, leading to enhanced antibacterial activity compared to proline and bromine ions. They observed morphological changes in *S. aureus* and *E. coli* strains exposed to the surface of the intrinsically antibacterial poly IL membrane.<sup>100</sup> As shown in Fig. 4C, Liu *et al.* prepared an efficient and robust antiseptic spray based on nonvolatile PILs, which indicated long-term antibacterial activity against both Gram-negative and Gram-positive bacteria on diverse materials, such as glass, PE, and cotton. The PIL with a longer side alkyl chain showed better antibacterial properties because of the stronger hydrophobic interactions with bacterial membranes caused by longer side chains, leading to membrane destruction.<sup>91</sup>

Compared with other antimicrobials, ILs exhibit multiple modes of action on bacterial cells. They can interact with and destroy bacterial membranes,<sup>83,101</sup> disrupt proteins and enzymes,<sup>102,103</sup> dysregulate bacterial metabolism,<sup>104,105</sup> induce oxidative stress response,<sup>106,107</sup> and cause DNA damage.<sup>108,109</sup> The tunability of ILs, which stems from the free combination of ions, allows for the adjustment of alkyl chain length and the selection of different ions to regulate the strength of antibacterial properties. This flexibility and operability enable targeted inhibition of bacterial colony growth, pathogen killing, and biological compatibility. However, there is a lack of a comprehensive understanding of the principles that underlie the antibacterial properties of ILs. For example, more systematic research is needed on the effects of functional groups, the length of anion chain, and the atomic number of heterocycles on the antibacterial activity of ILs is lacking. The mechanisms involved also need further investigation, *e.g.*, the different mechanisms of Gram-positive and Gram-negative bacteria with distinct structures. Moreover, existing solid antimicrobials, especially coated antimicrobials, have a short service life because of environmental factors, such as wear and wind. Innovative design, such as antibacterial spray, may overcome this limitation and has advantages in portability and ease of use, presenting a new avenue for the development of antimicrobial agents. Nevertheless, the long-term effectiveness, robustness, volatility, and biocompatibility of antibacterial agents require further exploration and design.

**3.1.2 ILs as antifungal agents.** Fungi are a significant cause of infections in humans and ILs have shown promising results in combating fungal infections. The mechanism of action of ILs against fungi has been a subject of significant interest. Suchodolski *et al.* showed that 25  $\mu\text{M}$  hydrophilic ILs removed 30–70% of the *Candida* biofilm, while 10  $\mu\text{M}$  ILs completely inhibited filamentation.<sup>110</sup> Then they used (1*R*,2*S*,5*R*)-(-)-menthol with three asymmetric carbon atoms and ILs, whose cations had optically active alcohol substituents belonging to chiral ILs (CILs), to form menthol-CILs. Menthol-CILs followed the “side chain effect,” which indicated that the longer alkyl chain displayed increasing antimicrobial ability. It was observed that the menthol-CILs caused damage to the cell plasma membrane and cell wall of *C. albicans* and detachment of the fungal cells after two-hour adhesion, which could be viewed as disinfectants, due to their compatibility and antifungal activity.<sup>75</sup> Reddy *et al.* found that 1-hexadecyl-3-methylimidazolium chloride ([C<sub>16</sub>MIM][Cl]) exhibited antifungal activity by inducing membrane permeabilization, causing leakage of intracellular material, generating ROS, and impairing mitochondrial function.<sup>111</sup>

ILs can remove the biofilm of fungi, inhibit their filamentation, dissolve chitin (component of fungal cell walls),<sup>112,113</sup> cause damage to the cell plasma and cell wall, and trigger detachment. For example, ILs have the capacity of damaging the *A. nidulans*' cell wall of both filaments<sup>114</sup> and fungal conidia.<sup>115</sup> Diego *et al.* investigated through reverse transcription PCR at a molecular level the expression of *A. nidulans* genes after exposure to IL alkyl-tributyl phosphonium chlorides (TP-IL) *in vivo*. They found that TP-ILs were involved in the synthesis of saturated fatty acids and ergosterol (upregulation of *fasA* and *HMGR1* genes), respectively. *A. nidulans* changed plasma membrane fluidity responsible for the membrane permeabilization evoked by TP-ILs. As an interrelationship between the cell membrane and the cell wall occurs, damage to the cell wall can also affect the organization of the plasma membrane (Fig. 4D).<sup>114</sup>

Various types of ILs have been found to have inhibitory effects on the growth of fungal colonies and biofilms. However, there were few research studies on the mechanism of ILs inhibiting the growth of fungi, and most lack a systematic and comparative approach. Most of the existing studies showed that a certain type of IL had resistance to the proliferation of certain bacteria or fungi; hence the resistance of ILs to bacteria and fungi varied with the species, yet the reasons had not been fully explained. Fungi are known to have more organelles than bacteria; therefore, is it better for them to overcome the inhibitory effects of ILs or does it increase the number of targets for ILs to attack and thus be susceptible to inhibition? In contrast, the main component of the bacterial cell wall is peptidoglycan, while the main component of fungal cell wall is chitin. Whether the ILs can be designed to target a structure (cell wall or organelle) to kill bacteria or fungi in a targeted way may be a research direction.

**3.1.3 ILs as anti-inflammatory agents.** Anti-inflammatory agents have been transformed into ILs, given ILs' diverse and



customizable nature. For instance, choline-based ILs paired with anions derived from phenolic acids have been discovered to exhibit anti-inflammatory and antioxidant properties. These ILs can be integrated into bacterial nanocellulose (BC) membranes to treat cutaneous diseases, demonstrating a sustained release on skin.<sup>76</sup> The low solubility of non-steroidal anti-inflammatory drugs (NSAIDs) limits their bioavailability, requiring high dosages to achieve therapeutic effects. However, this approach can lead to complications, involving gastrointestinal damage and acute renal dysfunction.<sup>116,117</sup> The ionization of approved drugs into ILs may substantially expand the formulation preparation method to meet the demand for medicines that address the above limitations. For instance, lidocaine was transformed into an IL to improve the transdermal penetration of etodolac, resulting in a dual-function active pharmaceutical ingredient (API)-IL.<sup>77</sup> Compared with uncharged NSAIDs (lidocaine-diclofenac vs. diclofenac), the water solubility of API-ILs increased up to 470-fold. To optimize the skin permeability of API-ILs, a bilayer wound dressing material was developed that induced an anti-inflammatory effect and showed biocompatibility.<sup>78</sup> In 2013, the only API-IL that reached the clinical trial stage was an IL consisting of the NSAID etodolac and lidocaine, which had an analgesic effect.<sup>118</sup> Unfortunately, the unsatisfactory results led to the termination of the trials in 2016.<sup>1</sup> Despite this setback, the groundbreaking clinical trials of ILs as drugs represent a significant step towards the biomedical application of these compounds.

The use of ILs in anti-inflammatory applications has several implications, such as the significant improvement of water solubility, dual-function drugs, and multi-layer drug dressings, all providing opportunities for progress. As the drug effects of API-ILs have developed, their properties and cost-effectiveness have improved. However, the results of clinical trials have prompted researchers to be more cautious in selecting and designing IL-based drugs to ensure their effectiveness and safety. In addition, the mechanisms underlying the anti-inflammatory effects of ILs have been scarcely explored. It is unclear whether ILs cause ROS production or stimulate stress responses. There are few studies on the direct effect of ILs on internal anti-inflammation in the body. Several important questions must be addressed before implementing the use of anti-inflammatory ILs in clinical practice. One of the primary concerns is the potential damage to healthy tissues and the consequent side effects. In addition, it is essential to determine, which inflammatory ILs are effective and which require modification. While the ionization of approved drugs is a promising approach, the anti-inflammatory activity of ILs remains poorly understood and the potential for adverse reactions is unknown. Significant challenges require further investigation to fully realize the medical and economic potential of ILs in anti-inflammatory applications.

**3.1.4 ILs as anticancer agents.** The treatment of cancer is a significant global challenge with drugs' low water solubility for anti-cancer applications being major concerns. ILs have unique advantages, such as high-water solubility, stability, and anti-cancer activity. By appropriately selecting cations and anions,

ILs can be tailored and customized for specific anticancer applications.<sup>119</sup> This section provides a detailed overview of how ILs derived from insoluble anticancer drugs can improve druggability and thus anti-cancer effects. In addition to improving the druggability of poorly soluble anticancer drugs, certain common ILs also have anti-cancer effects (see the top human body shown in Fig. 3).

Some common ILs, such as imidazole-based ILs, also have antitumor activity.  $[C_{16}MIM][Cl]$  can inhibit the growth of HeLa and human hepatocellular carcinoma (HepG2) cells, and reduce cell viability, damage to DNA, cause apoptosis, as well as alter the cell cycle.<sup>65,69</sup> From a molecular point of view,  $[C_{16}MIM][Cl]$  induced changes in the transcription of p53, Bax and Bcl-2, and genotoxicity, inhibited superoxide dismutase, imparted oxidative stress, decreased the glutathione content, and increased cellular malondialdehyde levels.<sup>65,69</sup> Pyridinium, ammonium, and other ILs have also been reported to have anticancer activity.<sup>120-122</sup> Aljuhani *et al.* showed anticancer activities of a series of pyridinium ILs on two lung cancer cell lines (A549 and H-1229), and the maximum rate of proliferation inhibition was 99.69%.<sup>123</sup> Bourakadi *et al.* evaluated the anti-tumor activity of a series of 3-methyl-1-alkyl-2-(thiazol-4-yl) benzimidazol-3-ium ILs against four human tumor cell lines: HT29 (colon), K652 (Leukemia), MDA-MB231, and SKBR3 (breast) and established the antitumor prospect of ILs based on thiabendazole. Furthermore, the alkyl chain length of cationic substitution played an important role on the cytotoxicity of these ILs.<sup>73</sup> Developing an IL-API that is non-toxic to normal cells remains a challenge. These results showed the broadly promising future for the application of ILs as possible anticancer agents in cancer treatment.

To achieve maximum efficacy with minimal side effects, one approach is to convert insoluble drugs that have already been approved into ILs. For example, methotrexate, choline, and amino acid ester have been transformed into ILs, namely tetrabutylphosphonium methotrexate ( $[TBP][MTX]$ ), L-phenylalanine ethyl ester methotrexate ( $[PheEt][MTX]$ ), and 1-ethyl-3-methylimidazolium methotrexate ( $[EMIM][MTX]$ ), as potential anticancer prodrugs. These ILs demonstrated more effective anticancer activity than free methotrexate against the human cervical carcinoma cell line (HeLa) cells (Fig. 4E).<sup>70</sup> Matrinium-based ILs, composed of cations derived from the Chinese herbal medicine matrine and a series of fatty acid anions with long chains rooted in vegetable oils, have demonstrated improved anticancer activities compared with free matrine. They also exhibited lower cytotoxicity on normal cells (L929) compared with tumor cells (HeLa and A549). Additionally,  $IC_{50}$  of matrinium-based ILs to HeLa and lung cancer cells A549 decreased quickly with elongation of the anionic alkyl chain length. This suggests that long alkyl chains with a polar head could alter cell integrity, rapidly disturb the lipid layer, cause membrane rupture, and ultimately lead to cell death.<sup>68</sup>

Functionalized ILs could also have antitumor effects. Ferrocene has sparked great research for cancer therapeutics due to the remarkable properties, such as exceptional cylindrical structure, fascinating redox properties, favorable



electrochemical behavior, and high stability.<sup>124–126</sup> A series of ILs comprising ferrocene (Fe-ILs) by quaternization of 1-*N*-(ferrocenylmethyl) imidazole, 1-*N*-(ferrocenylmethyl) benzimidazole, and 1-*N*-(ferrocenylmethyl)-1,2,4-triazole with long alkyl chain bromides demonstrated significant anticancer activity.<sup>66</sup> In particular, Fe-IL with the longest chain was found to be the most active with  $GI_{50} = 0.016 \mu\text{M}$ , which was less than that of the standard drug doxorubicin ( $GI_{50} = 0.018 \mu\text{M}$ ) against human breast cancer cells MCF-7. Fe-ILs displayed moderate to good selectivity (against MCF-7 cells over normal Vero cells) and pharmacological parameters, including oral activity, effortless absorption or translocation.<sup>66</sup> Hydrazones, existing in chemotherapeutic agents and many other drugs, attached to organic molecules could be applied to drug design relevant to anticancer activities.<sup>127–129</sup> Al-Sodies *et al.* designed and synthesized novel dicationic ILs (Di-ILs), which contained hydrazone as a spacer linking double pyridines with alkyl functionalized esters to form cations. In their experiment, the two most active Di-ILs showed 99.99% and 99.86% compromised cell ability against human lung cancer cells (A549 and H1299, respectively).<sup>72</sup>

ILs with anticancer activity seem to be a viable treatment option in the context of other anticancer therapies with many side effects and poor drug availability. ILs 'modified' by existing drugs may be readily accepted for use but their properties, such as metabolism, may also differ from those of the original drug, necessitating further research. Common and functionalized ILs with anticancer activity themselves are also very competitive in future anticancer applications, because of advantages such as tunability, favorable combination abilities, and good solubility. In addition to using the inherent anticancer activity of ILs, the introduction of functional groups with targeted ligands, prodrug activators, enzyme inhibitors, *etc.*, may allow for the integration of multiple therapeutic mechanisms to create a synergistic effect to enhance the overall treatment outcome.

**3.1.5 Other therapeutic components.** ILs have also been used in innovative technologies such as TE and organ prostheses, where they can serve as scaffolds for the growth and regeneration of tissues. TE is an emerging discipline to construct tissues or organs *in vitro* or *in vivo*. The first condition of materials used for TE is their biocompatibility. Certain ILs have biocompatibility and potential for the development of TE. For instance, Meira *et al.* took advantage of ILs and polyvinylidene fluoride (PVDF) to form electroactive scaffolds for muscle regeneration, which provided electrical stimuli and a biomimetic microenvironment. 1-Butyl-3-methylimidazolium chloride and choline dihydrogen phosphate ([BMIM][Cl] and [Ch][DHP]) were both able to induce PVDF to produce a  $\beta$ -phase suitable for TE. Moreover, IL-PVDF composite films had non-cytotoxicity capacity and myoblast cell line  $C_2C_{12}$  cell proliferation, accordingly allowing them to work in muscle TE.<sup>12</sup> Murugesan *et al.* utilized imidazolium ILs, such as [BMIM][PF<sub>6</sub>] and 1-butyl-3-methylimidazolium tetrafluoroborate ([BMIM][BF<sub>4</sub>]), to act as a templating agent and a doping source with N, F, and P or N, F, and B, and functionalized reduced graphene oxide (GO) using a simple hydrothermal method.<sup>130</sup> To our interest, IL-tri-doped GO was capable of stimulating human osteosarcoma cell attachment and

proliferation, which was a promising platform for bone TE.<sup>130</sup> Gu *et al.* designed and fabricated a bionic eye and utilized [BMIM][NTf<sub>2</sub>] and [BMIM][I] to fill the cavity, which acted as an electrolyte between the electrodes and mimicked the vitreous body of the human eye. This structure has potential for the treatment of blindness (Fig. 4F).<sup>92</sup>

In addition to good biocompatibility, ILs can also have anti-amyloidosis properties. Amyloidosis refers to the disease caused by the deposition of the abnormal protein amyloid in tissues or organs. The uniform and unstructured deposition of this protein leads to different degrees of dysfunction.<sup>131–133</sup> 1-Butyl-3-methylimidazolium bromide ([BMIM][Br]) has been proved to have anti-amyloidogenic activity. Atomic force microscopy (AFM) imaging unequivocally showed that the IL significantly attenuated fibrillogenesis in lysozymes.<sup>134</sup> These results facilitated the development of more efficient therapeutics for amyloidosis.

The versatility of ILs has made them valuable in disease treatment by enhancing drug solubility and serving as active ingredients. ILs have been utilized in many therapeutic fields (*e.g.*, antibacterial, antifungal, anti-inflammatory, and anti-cancer); yet there are still challenges to be addressed, such as ILs' stability, safety, and efficacy *in vivo*. As aforementioned, the ionization of approved drugs (*e.g.*, lidocaine-diclofenac) can improve the solubility and bioavailability, which retain the potential for multiple therapeutic effects but avoid the *de novo* design. In this sense, a considerable amount of IL-based drugs is under developed. Given the ILs' vast diversity structures with nearly  $10^{18}$ , it is also a complex and huge labor-intensive task to investigate the therapeutic potential of each IL *via* practical experiments. In order to rapidly and rationally design these ILs, the assistance of artificial intelligence (AI) is highly awaited. By machine learning and data mining of the existing experimental evidence, especially on the therapeutic effect and ILs' components/physicochemical properties (anions, cations, side chains, functional groups, structures, *etc.*), the key parameters can be predicted and incorporated into IL-based drug formulations to achieve a desirable therapeutic effect.

### 3.2 Therapeutic mechanisms

To further advance the potential of ILs as promising drug candidates for disease treatment, a better understanding of the interaction mechanism between cells and ILs is essential. Due to the strong interaction among anions, cations, and other molecules, ILs have impacts on different degrees of life substances, from single proteins to intricate multicellular organisms.<sup>7,135–139</sup> The interaction of ILs with biological systems has opened up a broad prospect for their application in biomedicine. In this section, we summarize the effects of ILs on cell membranes, organelles, nucleic acids and proteins.<sup>106,139–142</sup> Simultaneously, a detailed analysis will be conducted on the relationship between the structure of ILs and their interaction with organisms.

**3.2.1 Interactions between ILs and cell membranes.** The initial interaction of ILs with cell membranes at the molecular level is crucial. As the interface between the inner and outer





environment of the cell, cell membranes are vital for the cell's independent existence and serve as the first protective barrier against foreign substances. The affinity and permeability of cell membranes and ILs are pre-requisites for ILs' important effects on cells. If ILs are developed as drugs, it is necessary to fully comprehend the relationship between the different ionic structures of ILs and cell membranes to provide reliable design guidelines. In this section, we introduce the mechanisms and influencing conditions of ILs acting on cell membranes.

At the forefront of the interaction between ILs and cell membranes is the interaction between ILs and lipid bilayers. This is because lipid bilayers are the primary components and structures of cell membranes. The lipid membrane is comprised of phosphatidylcholine, which features a zwitterionic head group (net charge of zero) that facilitates electrostatic interactions and fatty acid tails in the inner region of the bilayer that provide hydrophobic interactions.<sup>143</sup> ILs can control hydrophilic and hydrophobic characters by selecting the radius of their ionic moieties and size of their neutral parts to interact with bio-molecules. In fact, most ILs and cationic surfactants (in terms of structure, inherent charge, and function) have similar properties and can be adsorbed onto the surface of organisms, thereby increasing the permeability of the cell membrane.<sup>144,145</sup>

Previous studies have suggested that the interaction between ILs and cell membranes is influenced by the alkyl chain length of the ILs. The lipid bilayer is usually made of biomimetic membranes according to experiments, such as dioleoyl phosphatidylcholine (DOPC), which typically undergoes dissolution, drying, rehydration, vortex formation, and ultrasound treatment. Galluzzi *et al.* demonstrated that the length of the alkyl chain of the IL cation dominated the strength of the IL and lipid bilayer interaction and observed the interaction between lipid bilayers deposited on mica surfaces and ILs through atomic force microscopy.<sup>146</sup> An experiment revealed that 1-hexyl-3-methylimidazolium acetate ([HMIM][OAc]) could be inserted into the lipid bilayer in the gel state, causing a more marked influence on the lipid bilayer than 1-butyl-3-methylimidazolium acetate ([BMIM][OAc]).<sup>147</sup> The permeation of the IL cation into the lipid membrane led to the reorganization and softening of the bilayer, ultimately forming an IL/lipid complex. Furthermore, MD simulations revealed that the hydrophobicity of the IL cation, associated with its chain length, was the primary driver of its insertion into the lipid bilayer.<sup>145</sup>

Moreover, the interaction between ILs and lipid bilayers is also influenced by the ILs' cationic head groups, number of substituents, and anions. ILs' head-group structures have a strong dependence on the permeability of the lipid bilayer (Fig. 5A).<sup>148</sup> Kaur *et al.* investigated the impact of six cationic head groups on lipid bilayers using solid-state NMR spectroscopy. Size, hydrophobicity, and delocalized and unshielded charges of the positively charged head-groups affected the degree of influence on lipid bilayers.<sup>148</sup> In another study, they used double-chained 1-alkyl-3-octylimidazolium cations ([C<sub>n</sub>C<sub>8</sub>IM]<sup>+</sup>, *n* = 2, 4, 6, 8, 10, and 12) to evaluate membrane

permeability through fluorescence-based dye leakage assays, which increased with the growth of the alkyl chain on N1 atoms, whereas double-chained ILs had lower permeability compared to single chain ILs with a similar carbon atomic number (Fig. 5B).<sup>149</sup> Kumari *et al.* determined that anions were the main components causing the observed structural disturbances of lipid bilayer using MD simulations.<sup>150</sup> A recent report discussed the relationship and mechanism between IL's molecular size and membrane damage. Xu's team found that ILs mainly interacted with negatively charged phosphate heads in lipid bilayers using antibacterial tests, fluorescent tracing, morphology observations, molecular biology, and MD simulations.<sup>151</sup> The ability to insert into the bilayer membrane depended on the molecular size and disturbance of the membrane of ILs. Specifically, ILs with relatively short carbon chains could pass through the cell membrane causing membrane thinning, while ILs with long carbon chains remained in the cell membrane to disturb it. However, the medium-length carbon chain ILs were similar to the length of the bilayer membrane and had little impact on the cell membrane (Fig. 5C).<sup>151</sup>

While many simulations have provided insights into the mechanism of cell membrane destruction by ILs, detailed experimental data are still lacking. Currently, the mainstream approach is to study how ILs' alkyl chain insertion, intercalation of the anionic rings, or disturbance of cationic head groups change the phospholipid bilayer structure and mechanical elastic properties. Currently, most of the studies on cell membrane toxicity of ILs focus on imidazole-ILs, limiting the study of cytotoxicity on cell membranes. In addition, biomimetic membranes are the main model structure for the study of IL's action on cell membranes. Although biomimetic membranes can partially mimic the structure of phospholipid bilayers, they fall short in replicating the full complexity and functionality of natural cell membranes. We speculate whether ILs as ionic compounds can also affect proteins and ion channels or the motion track of ions on cell membranes given the interaction between charged ions. Overall, studying the interactions between ILs and cell membranes in living cells is a complex area of research that requires careful consideration of experimental design and safety measures to ensure reliable and meaningful results.

**3.2.2 Interactions between ILs and cell organelles.** ILs have the effect of killing cancer cells. Thus, the interaction mode between ILs and organelles and the impact on organelles are crucial for the research and development of ILs as targeted anticancer agents. In particular, understanding the mode of interaction between ILs and organelles such as lysosomes and mitochondria is important for the development of ILs as targeted anticancer agents. Studies have found that ILs can alter and damage the structure of lysosomes. For instance, Bansode *et al.* found that ferrocene-tethered ILs could inhibit the breast cancer cell MCF-7 *via* inhibition of lysosomal peptidase cathepsin B. During this process, aromatic rings and side chains were found to play a regulatory role in the anticancer activity of these ILs.<sup>66</sup> By comparing [BMIM][BF<sub>4</sub>] and 1-octyl-3-methylimidazolium tetrafluoroborate ([OMIM][BF<sub>4</sub>]) in cells,





**Fig. 5** ILs acting on living organisms: (A) schematic models of different ILs' head-group size, hydrophobicity, and charge delocalization impacting the structure of 2-oleoyl-1-palmitoyl-*sn*-glycero-3-phosphocholine (POPC) bilayer. Black wavy lines: alkyl chains in lipids and cations, grey filled circles: glycerol moieties in the lipid head-groups, blue and red filled circles connected with black lines: phosphocholine dipoles, and red circles: head-groups of cations intercalated in lipid molecules. Reproduced with permission from ref. 148. Copyright 2020 Elsevier. (B) The leakage kinetics of calcein dye from POPC and 2-oleoyl-1-palmitoyl-*sn*-glycero-3-phosphoglycerol (POPG) large unilamellar vesicles and the regular model of membrane permeability associated with ILs' cations. Reproduced with permission from ref. 149. Copyright 2021 American Chemical Society. (C) The membrane damage mechanism of ILs with different chain lengths on Gram-negative bacteria. Reproduced with permission from ref. 151. Copyright 2020 American Chemical Society. (D) Methylimidazolium ILs affecting the mitochondrial electron transport chain in mammalian cells. Reproduced with permission from ref. 152. Copyright 2020 Elsevier. (E) The effects of [C<sub>10</sub>MIM][Cl] on mitochondria of HeLa cells with the original TEM images (top) and zoomed TEM images (bottom). Reproduced with permission from ref. 141. Copyright 2021 Elsevier. (F) Distribution map of the IL interaction with DNA. Cyan: DNA, red: DNA phosphates, white: IL cations, and blue: ring nitrogen of IL cations. Reproduced with permission from ref. 153. Copyright 2012 American Chemical Society. (G) The mechanism for ILs' long hydrocarbon chains of anions preventing a fungicide from destroying structural DNA. Reproduced with permission from ref. 154. Copyright 2020 American Chemical Society. (H) The formation mechanism for bovine serum albumin (BSA) amyloid fiber in the presence of [EMIM][BF<sub>4</sub>] (2–10 v/v%). Reproduced with permission from ref. 155. Copyright 2021 American Chemical Society. (I) The effect and relationship between the length of alkyl chain of anion (left) and cation (right) on proteins. Reproduced with permission from ref. 156 and 157. Copyright 2018 Royal Society of Chemistry and 2020 American Chemical Society.



Tsarpali *et al.* found that ILs had the ability to cause lysosomal membrane damage.<sup>144</sup> The magnitude of toxicity was found to be dependent on the length of the alkyl chain and lipophilicity of ILs.<sup>144</sup>

At present, most studies on the toxicity of ILs to organelles focus on mitochondria.<sup>158</sup> Methylimidazolium ILs can act as mitochondrial electron acceptors and longer chain ILs may act on the inner mitochondrial membrane affecting mitochondrial endometrial electron transmission and producing excess ROS (Fig. 5D).<sup>152</sup> Research suggested that longer chain methylimidazolium liquids were toxic to sensitive liver progenitor cells because they both readily integrated within the inner mitochondrial membrane, accepting electrons from the electron chain and leading to oxidative stress. 1-Decyl-3-methylimidazolium chloride ([C<sub>10</sub>MIM][Cl]) caused mitochondrial swelling, vacuolation and cristae rupture, resulting in excessive ROS levels that ultimately damaged the mitochondrial membrane potential and induced cell apoptosis (Fig. 5E).<sup>141</sup>

Although our understanding only involves a few organelles like mitochondria and lysosomes, it shows the mode of action of ILs on cytotoxicity and highlights the lack of cytotoxic mechanism of ILs at this stage. Understanding ILs' current mechanism of action on organelles is valuable for the development of targeted ILs that are tailored to a specific organelle. For example, lysosomes are known to have an acidic environment, making them attractive targets for drug delivery. In this regard, ILs can be designed into specific structures to neutralize the acidity of the lysosome and disrupt its membrane, thereby enabling the drug to escape and reach its target site.

**3.2.3 Interactions between ILs and nucleic acids.** Nucleic acid, the most crucial substance among biological molecules, possesses a significant charge per unit length on its chain due to anionic polyelectrolytes. This inherent charge enables positive cations in ILs to interact with nucleic acids, forming ion pairs or complexes. However, it is important to note that the effects of ILs on nucleic acids can vary depending on their composition, structure, and properties. For instance, Li *et al.* investigated the toxicity of three ILs on zebrafish, namely, 1-aminoethyl-3-methylimidazolium tetrafluoroborate ([C<sub>2</sub>NH<sub>2</sub>-MIm][BF<sub>4</sub>]), 1-methoxyethyl-3-methylimidazolium tetrafluoroborate ([MOEMIm][BF<sub>4</sub>]), and 1-hydroxyethyl-3-methylimidazolium tetrafluoroborate ([HOEMIm][BF<sub>4</sub>]). The results revealed that as the length of the cationic side chains increased, the toxicity of the ILs gradually intensified.<sup>159</sup>

Simulation methods are mainly used to study the interaction mechanism between ILs and nucleic acids. According to current reports, ILs mainly combine with nucleic acid grooves through H-bonds and hydrophobic interaction, giving origin to the groove binding mechanism. Although RNA and DNA are similar in structure, DNA is known for its greater stability, which has led to its prominence in investigations involving IL interactions. Rezki *et al.* demonstrated the interactions of imidazole ILs containing fluorine with DNA *via* H-bonds through modeling studies.<sup>160</sup> Choline ions were stably combined with DNA atoms through multiple H-bonding networks from a microscopic viewpoint using MD simulations.<sup>161</sup> Al-Sodies *et al.* found that ILs and DNA had good binding

tendencies in the outer groove.<sup>72</sup> The rod-like structure of imidazolium-based ILs exhibited a higher propensity to bind to the minor groove of calf thymus DNA, while the interaction of individual nucleic acid bases and imidazolium-based ILs confirmed the increasing tendency to bind to different bases in the following order: guanine, cytosine, thymine, uracil, and adenine.<sup>162</sup> Nakano *et al.* demonstrated that multiple H-bonds played a significant role in the interaction between choline ions and DNA.<sup>161</sup> Wang *et al.* found that the electrostatic interaction between the cationic head group of ILs and DNA and the hydrophobic interaction between the hydrocarbon chain of ILs and DNA predominated.<sup>163</sup> Fig. 5F shows the distribution map of IL's cations in DNA molecules.<sup>153</sup>

The interaction between ILs and nucleic acids has garnered significant attention in current research. Studies have demonstrated that while certain ILs can cause damage to nucleic acids, they also possess the capability to counteract the irreversible damage inflicted by toxic substances. For example, Sarkar and Singh prevented DNA damage from fungicide by adding ILs possessing anions with long hydrophobic chains (Fig. 5G).<sup>154</sup> Long hydrophobic chain anions ILs combined with DNA through micelle-like structures prevented the combination of fungicide with DNA, and reversed the damage of DNA at the same time. Meanwhile, the application of ILs in nucleic acid delivery has developed rapidly, providing infinite possibilities for the application of ILs in biomedicine.

**3.2.4 Interactions between ILs and proteins.** ILs have been reported as novel and promising amphiphilic compounds that can replace water and volatile organic compounds such as solvents or additives to affect protein stability or activity.<sup>156</sup> As the basic organic matter of cells, the activity and state of proteins are closely related to life activities. Many active sites of proteins can combine with biological molecules, such as lipids and sugars and interact with water to diversify the behavior and realize the foundation of life. They are usually charged, depending on the varying chemical or physical conditions, such as pH, temperature, and pressure. Many ILs are similar to cationic surfactants,<sup>106,164</sup> which can destroy proteins.

The interactions between ILs and proteins depend on H-bonds, van der Waals force, hydrophobic interactions, *etc.*<sup>155,165–168</sup> For instance, anions of choline-based ILs choline iodide, choline bitartrate, and choline dihydrogen citrate ([Ch][I], [Ch][Bit] and [Ch][Dhc]) could spontaneously combine with the residues of bovine serum albumin (BSA) by H-bonds and van der Waals force, changing the natural structure of BSA significantly.<sup>165</sup> Choline geranic acid ILs (CAGE) could inhibit human neutrophil elastase at low concentrations by disrupting the hydrophobic effect.<sup>169</sup> Besides, the addition of ILs can change the pH of the environment and denature proteins. [EMIM][BF<sub>4</sub>] could cause conformational changes of BSA, resulting in the formation of amyloid fibers. The time-dependent hydrolysis of [EMIM][BF<sub>4</sub>] changes the pH of the solution. The synergism of pH and the electrostatic interaction of IL with BSA led to amyloid fibrils (Fig. 5H).<sup>155</sup>

The interactions between ILs and proteins depend on the structure of ILs. The ILs' anionic hydrophobic structure can





interact with proteins and lead to complex behaviors between ILs and proteins.<sup>157,170,171</sup> For example, the interaction between choline-based ILs and BSA varied greatly due to different anions.<sup>165</sup> Briefly, choline chloride ([Ch][Cl]) had no obvious effect on the conformation of BSA, while choline bromide [Ch][Br] changed its conformation slightly. In the presence of [Ch][I], [Ch][Bit] and [Ch][Dhc], the conformation of BSA changed significantly. The quenching mechanism of [Ch][Bit] and [Ch][Dhc] was a static quenching process, while [Ch][I] had a combined mechanism of charge transfer quenching and static quenching. Singh *et al.* demonstrated that the interaction of lysozyme (LYZ) with ILs was dependent on the molecular structure of the anionic counterpart of the ILs, with choline deoxycholate ([Ch][Doc]) showing greater involvement in bulk complexation compared with choline lauryl sarcosinate ([Ch][Sar]).<sup>171</sup> [Ch][Doc] stabilized the secondary structure of LYZ *via* hydrophobic–hydrophilic interactions, while [Doc] adsorption onto LYZ provided stability through polar interactions. Conversely, [Sar] induced greater unfolding of LYZ, especially at higher concentrations, because of its flexibility and single-chain system with an amide moiety. What is more, the overall binding affinity between ILs and proteins increased with the length of the alkyl chain of the anion and cation of ILs. Fig. 5I shows the effect and relationship between the length of the alkyl chain of the anion and cation on proteins.<sup>156,157</sup>

Pabbathi and Samanta researched the effects of two ILs with different alkyl chain lengths on protein stability.<sup>156</sup> The long chain ILs interacted with the protein hydrophobic region and destroyed the tertiary structure of Cyt-*c*. Conversely, the short chain ILs had a weaker effect on the Cyt-*c* structure because of reduced hydrophobicity compared with that of long chain ILs. The inhibitory and disturbing effects of ILs on proteins make them promising antibacterial agents. Bacterial cell walls and membranes contain important proteins that can be denatured or deleted through reasonable design and addition of ILs. The current models and experimental conditions for investigating the interaction between ILs and proteins are often constrained and may not comprehensively capture the complexity of the system. Therefore, it is necessary to develop a research methodology that integrates both experimental and computational approaches, along with high-throughput screening methods.

Notably, although ILs have made substantial progress in exploration of ILs in biomedicine applications, further research is still needed to elucidate their underlying mechanisms. Firstly, investigations into the therapeutic mechanisms of ILs primarily concentrate on the alkyl side chains (*e.g.*, long side chain-derived antibacterial effect). The exploration of other structures of ILs on therapeutic mechanisms, such as anions and cations, remains limited. It is crucial to broaden the scope of research to encompass the effects of various ILs' structures on therapeutic mechanisms. Secondly, the absence of standardized protocols for assessing the relationship between the drug efficacy and the mechanisms might also hinder the comparability of different studies and limit the generalizability of their findings. Thirdly, *in vivo* research experiments mostly depend

on the model organism or rodent animals, which could be expanded (to big animal beagles, pigs, *etc.*) to establish a multi-level and full chain biological evaluation system for the safety of ILs.

## 4 Biomedical aids

### 4.1 Application of ILs in pharmaceutical engineering

ILs are called 'designer solvents' in synthetic strategies because of their adjustable structure and ability to dissolve a wide range of compounds.<sup>172</sup> ILs have ideal properties through rational design, such as broad solubility, unique H-bond system, negligible vapor pressure, and stable chemical properties, making them attractive alternatives to traditional extractants and catalysts in drug separation and synthesis. ILs also have high selectivity, making them an attractive option for separation and purification processes. In addition, they can be used as reaction catalysts in drug synthesis, offering advantages such as increased reaction rates, improved selectivity, and improved product purity. This section provides an overview of the use of ILs in drug separation as extractants and drug synthesis as catalysts.

**4.1.1 ILs as extractants in drug separation.** ILs are emerging as excellent extractive solvents for the separation and purification of drug components because of their excellent solubility, negligible volatility, and stability. Many volatile, flammable, or even toxic organic solvents are often consumed in traditional drug extraction processes. However, these typically create pollution in the environment, demonstrate unsatisfactory extraction efficiency, and complicate the post-treatment of the extracted drugs.<sup>173,174</sup> ILs have been extensively investigated in the extraction of natural products from plants given their ability to optimize the extraction of bioactive compounds such as alkaloids, terpenoids, flavonoids, phenolic acids, aromatic compounds, and lipids.<sup>175–180</sup> Compared with traditional solvent-based methods, IL-based extraction approaches have exhibited superior extraction yields and selectivity. Moreover, the recoverability and reusability of ILs contribute to their reduced environmental impact and cost-effectiveness. ILs are now investigated as alternative compounds to conventional solvent extraction, supercritical fluid extraction, and cloud point and to solve energy consumption and environmental impact problems. This section will introduce three common extraction methods: IL extraction, ILs with microwave-assisted or ultrasound irradiation-assisted extraction.

ILs can be used as direct extractants to extract active pharmaceutical components because of interactions between ILs and other substances. Compared with commonly used organic extractants, ILs offer clear advantages in terms of extraction efficiency, sample pretreatment, and environmental impact. For example, using ILs to extract and recover lipids from microalgae and yeast after fermentation could result in higher extraction efficiency, shorter processing time, lower energy consumption, and the ability to reuse the ILs, which could lead to significant improvements in economic efficiency.<sup>180</sup>



Gökdemir *et al.* used [BMIM][NTf<sub>2</sub>] as an alternative green solvent to extract curcumin from turmeric, with a maximum yield extraction of 2.94% under optimal conditions.<sup>181</sup> Ji *et al.* showed how pure ILs could act as an efficient and selective extracting agent for minor anticancer prenylated flavonoids from a herbal medicine.<sup>182</sup> Considering the H-bond interactions between [OMIM][BF<sub>4</sub>] and prenylated flavonoids, the extraction yield of prenylated flavonoids was as high as 78.92% using reversed-phase solid phase extraction from [OMIM][BF<sub>4</sub>].<sup>182</sup>

The interaction between ILs and substrates is a key consideration for extraction.<sup>183</sup> Considering the ILs' anion and cation tunability, specific properties of fluids can be designed to ensure that the target-active molecules are highly solvated to improve the extraction efficiency. In an IL-based aqueous two-phase system of separation of acteoside from *Cistanche tubulosa*, [BMIM][BF<sub>4</sub>] and (NH<sub>4</sub>)<sub>2</sub>SO<sub>4</sub> had collaborative extraction roles. Specifically, the high polarity of [BMIM][BF<sub>4</sub>] provided multi-H-bond receptors for acteoside, whereas (NH<sub>4</sub>)<sub>2</sub>SO<sub>4</sub> made acteoside stable by creating a weak acidic microenvironment and reducing solubility of acteoside in the salt phase.<sup>184</sup> In another report, the IL-based surfactant-free microemulsion system consisting of [HMIM][BF<sub>4</sub>], 1,2-propanediol, and H<sub>2</sub>O was used to extract and separate hydrophilic (phenolic acids) and lipophilic compounds (alkaloids) from *Camptotheca*

*acuminata*.<sup>176</sup> van der Waals forces and H-bonds were supposed to be the main force between IL-based microemulsion and targeted compounds.

ILs are more environment friendly, with greater extraction efficiency and recycling advantages compared with traditional extractants. However, there are still many problems in the process of IL extraction. A key challenge in the extraction of bioactive compounds using ILs is their high viscosity, which can lead to lower extraction efficiency and slower mass transfer rates. To solve this issue, microwave-assisted extraction (MAE) and ultrasound-assisted extraction (UAE) have been developed. These methods employ high-frequency electromagnetic waves or sound waves to improve the mass transfer rate and extraction efficiency of IL-based extraction processes. Fig. 6A illustrates the extraction process for bioactive compounds using ILs assisted by either microwave or ultrasound.

ILs have emerged as a promising microextraction technology because of their unique ability to absorb microwave energy and convert it into heat. Additionally, because ILs are composed of cations and anions, high polar ILs can be reasonably designed to absorb and transfer microwave energy effectively.<sup>187</sup> MAE can break the cytoderm and heat cells to accelerate the dissolution of intracellular effective components.<sup>135</sup> Therefore, IL-MAE can depend on cell penetration and selective heating to

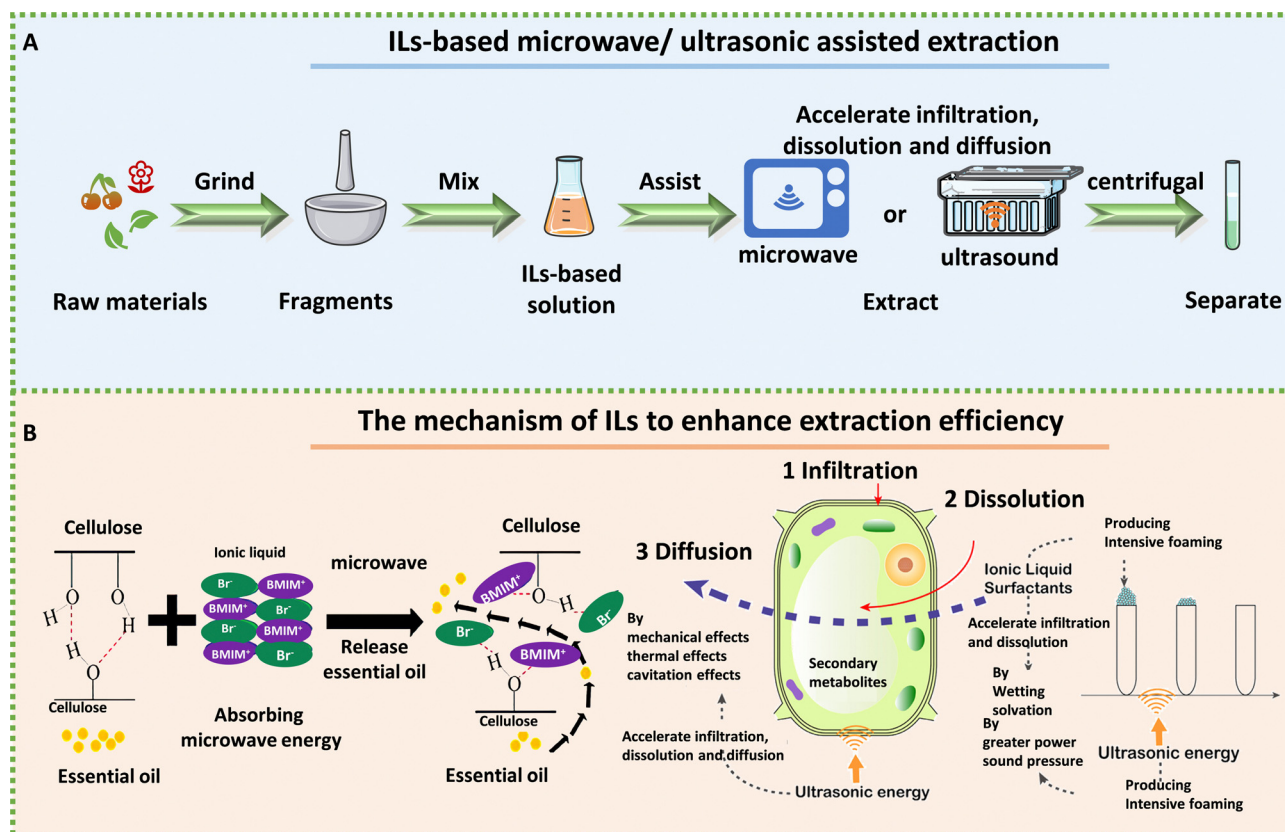


Fig. 6 The process and mechanism of IL-based microwave- and ultrasonic-assisted extraction technology. A: Schematic extraction of biologically active ingredients by IL-assisted with microwave or ultrasound. B: Mechanism of ILs to enhance efficiency for extracting essential oil from *Foeniculum fructus* in IL-based microwave system (left) and psoralen and isopsoralen from *Psoralea corylifolia* seeds in IL-based ultrasonic extraction (right). Reproduced with permission from ref. 185 and 186. Copyright 2021 by the authors, licensee MDPI and 2020 Elsevier.



help ILs in extracting drug components from plant raw materials. For example, Komaty *et al.* used ILs with MAE to extract atranorin, methyl- $\beta$ -orcinol carboxylate, fumarprotocetraric acid and physodic acid from lichens more rapidly than when using conventional heating.<sup>188</sup> Chen *et al.* successfully used magnetic 1-butyl-3-methylimidazolium tetrachloroferrate ([OMIM][FeCl<sub>4</sub>])-microwave to extract essential oil from lavender.<sup>189</sup> Shi *et al.* employed ILs and MAE-assisted extraction to extract essential oil from *Foeniculi fructus*, which significantly improved the extraction efficiency. MAE had been shown to enhance the diffusion of essential oils from plants into ILs. The process of interaction between ILs and cellulose had also been emphasized, wherein non-covalent interactions (H-bonds and van der Waals forces) between the ILs and cellulose lead to the breakdown of the H-bonds' cellulose structure.<sup>185</sup>

IL-based UAE extraction has been identified as an efficient technique to facilitate natural product extraction and increased yield. Compared with traditional extraction, UAE-assisted extraction has less solvent consumption and shorter extraction time.<sup>190</sup> Ultrasound can damage the plant tissue and accelerate the penetration of solvents. Sui *et al.* utilized IL-based ultrasonic extraction of psoralen and isopsoralen from *Psoralea corylifolia* seeds through infiltration, dissolution, and defoaming; long alkyl-chain ILs such as [C<sub>10</sub>MIM][Br] had better extraction efficiency.<sup>186</sup> UAE played three promoting roles in the system (vibration, thermal, and cavitation effects), improving the mass transfer efficiency, increasing the contact area, and enhancing the solubility of psoralen and isopsoralen. Sukor *et al.* found that the extraction efficiency of the UAE system was greatly improved after the addition of ILs.<sup>191</sup> They believed that the cavitation effect after ultrasound and the special properties of 1-butyl-3-methylimidazolium bis(trifluoromethylsulfonyl)imide ([BMIM][NTf<sub>2</sub>]) synergistically improved the extraction efficiency. Sun *et al.* established a simple, rapid, and green system consisting of ultrasound-[BMIM][Br] solid-liquid extraction coupled with aqueous two-phase extraction high-performance liquid chromatography to extract naphthoquinone pigments in *Arnebia euchroma* (Royle) Johnst.<sup>192</sup> Furthermore, Li *et al.* used an IL-based ultrasonic-assisted method to extract ganoderic acid A and D from *Ganoderma lucidum*, with an extraction yield of 3.31 mg g<sup>-1</sup>, which was much higher than that obtained using methanol as solvent.<sup>193</sup> They also found that the extraction efficiency was related to the structure of the IL based on the comparison of five ILs, including [BMIM][Br], [BMIM][BF<sub>4</sub>], [BMIM][PF<sub>6</sub>], 1-hexyl-3-methylimidazolium bromide ([HMIM][Br]), and 1-octyl-3-methylimidazolium bromide ([OMIM][Br]). The extraction rate related to the alkyl chain length impacted the hydrophobicity, van der Waals force, and viscosity, while the anions interacted with the hydroxyl groups of the target compounds through the H-bonds,  $\pi$ - $\pi$  conjugation, and ion/charge forces.<sup>193</sup>

Microwave and ultrasonic assisted-IL extractions improve the extraction efficiency through a fast and effectively enhanced process (Fig. 6B). In addition to the two IL-based external field assisted extraction methods, other IL-assisted extraction methods exist, such as IL-heating extraction,<sup>194</sup> IL-based pulsed

electric fields<sup>195</sup> and IL-based pressurized liquid extraction.<sup>196</sup> However, these methods may have drawbacks, such as increased energy requirements or the need for expensive and high-security equipment. What is more, most researchers believe that the combination of ILs and extracted substances is driven by the H-bonds, but there is limited detailed mechanisms explaining how microwave and ultrasound irradiation improve the extraction efficiency. Therefore, a better understanding of the extraction mechanisms for targeted biological complexes is needed to be explored. In addition, when separating the bioactive components extracted by ILs, organic solvents are often needed for back extraction to recover the target compounds in the treatment process, hindering the 'green' features of the separation process. The problems of IL residues in biologically active ingredients, and safety, also need to be further considered.

**4.1.2 IL catalysts in drug synthesis.** The adjustment of anions, cations, and substituents for functional design makes ILs excellent catalysts in a reaction process. H-bonds with other substances and properties such as amphiphathy and acid-base make them excellent catalysts in the reaction process.<sup>197,198</sup> IL-based catalysts provide numerous benefits compared with traditional catalysts, such as their high adjustability and recyclability, reduced metal and halogen pollution, and enhanced separation between the catalyst and the product. In addition, IL-based catalytic systems offer a notable advantage in terms of reducing neutralization after the reaction, thereby enhancing their sustainability.

Researchers have reported IL applications in various chemical processes, *e.g.*, as catalysts related to the production of drugs. These include antimicrobial, antiviral, antimalarial, antitumor, and other drug agents over the past few decades, *e.g.*, [L-prolinium chloride][1-methylimidazolium-3-sulfonate] as the catalyst to synthesize antibacterial hydrazono-4-thiazolidinones.<sup>199</sup> Sulfonic acid-functionalized ILs were utilized for catalytic synthesis of pyrano[3,2-*c*]coumarin derivatives and C3-substituted 4-hydroxycoumarins.<sup>200</sup> IL cations had a strong influence on the catalytic activity in the synthesis of quinazoline-2,4(1*H*,3*H*)-diones, in which the H-bonds formed by the cations and the alkalinity of the cations affected the reaction.<sup>201</sup> Wang *et al.* proposed IL catalytic mechanisms for the reactions of pyrano[3,2-*c*]coumarin derivatives and C3-substituted 4-hydroxycoumarins. They believed that the propargylic or allenic carbocation and H-bond effects between the catalysts and the substrates were the reason for the process of alkylation and cyclization.<sup>200</sup> Table 1 shows examples of ILs used as catalysts in drug synthesis.

ILs play an important role in drug synthesis as catalysts and offer numerous advantages over traditional synthesis techniques (*e.g.*, excellent selectivity). However, several challenges require attention and resolution, such as the residual problem of ILs in drugs in the post-treatment process, environmental fate, and safety issues. Cross disciplinary collaborative research may be helpful in addressing these issues to elucidate the mechanisms underlying the interactions between ILs and biological systems, shedding light on their potential benefits or risks.





Table 1 Ionic liquids (ILs) as catalysts in drug synthesis

ILs	Drugs	Activities	Ref.
Piperidinium acetate	Spiro-piperidine derivatives	Antileishmanial	202
[DBU][Ac]	Triazole-tetrazole conjugates	Anthelmintic	203
[Trps][OTs]	Aspirin	Anti-inflammatory	204
[BMIM][Br]	2-(1 <i>H</i> -Benzimidazol-2-yl) phenol	Anticancer	205
	2-(Thiophen-2-yl)-1 <i>H</i> -benzimidazole		
[BMIM][BF <sub>4</sub> ]	Pyrazolo quinoline derivatives	Anti-inflammatory and antioxidant	206
Hexamethylenetetramine based IL	Tetrazolo[1,5- <i>a</i> ] pyrimidine-6-carbonitriles	Antiproliferation and antitumor	207
[MerDABCO-SO <sub>3</sub> H][Cl]	Pyrazolopyranopyrimidines	Antimicrobial and antioxidant	208
Brønsted acidic dicationic IL	4,4' (Arylmethylene)bis(3-methyl-1-phenyl-1 <i>H</i> -pyrazol-5-ol)	Antiviral, antibacterial, and antifungal	209

The emergence of green chemistry has significantly increased the interest in ILs within the domain of pharmaceutical engineering. ILs have gained recognition as extractants for drug separation and catalysts in drug synthesis and for their potential in synthetic biology. ILs offer unique properties, including negligible vapor pressure, high thermal stability, and adjustable solvation capabilities, making them highly attractive for applications in the field of synthetic biology. For instance, ILs can be employed as reaction media during the process of recombinant DNA and modular enzyme assembly. By deviating from conventional drug production systems, ILs have the potential to serve as extractants or catalysts for the design and synthesis of biological molecules, ultimately leading to the development of novel drugs.

#### 4.2 Application of ILs in disease diagnosis

The unique ion-free composition of ILs consisting only of ions and their fascinating thermal, electrical, physical, and chemical properties aroused enormous interest in disease diagnosis. Thus far, there have been many researchers focusing on the application of ILs in diagnostics, including biosensing and imaging. A growing body of research demonstrates that IL

can be used not only as sensors to improve performance (Fig. 7A), but also as electrodes, hence they are involved in the diagnosis of the disease and improve the diagnostic efficiency.

**4.2.1 IL-based sensors to diagnose physical diseases.** ILs possess superior properties, including an adjustable structure, excellent electrochemical performance, and potential biological compatibility, making them ideal for medical diagnosis *via* the development of bio-electrochemical sensors. These sensors may provide high anti-interference ability, sensitivity, repeatability, and a satisfactory detection range. Chemicals, such as glucose and proteins, play a crucial role in maintaining normal body metabolism and their rapid and efficient testing with ILs can aid in the diagnosis of diseases. ILs have been extensively studied for the diagnosis of diseases, including kidney diseases, diabetes, gout, cancer, mental illness, depression, and Alzheimer's disease.

IL-based sensors have shown potential in diagnosing kidney diseases by detecting the levels of biomarkers such as human serum albumin (HSA) and creatinine. Gao *et al.* developed a fluorescent sensor using a luminogen, decorated with tetraphenylethene (TPE) and 1-carboxymethyl-3-methyl-imidazolium

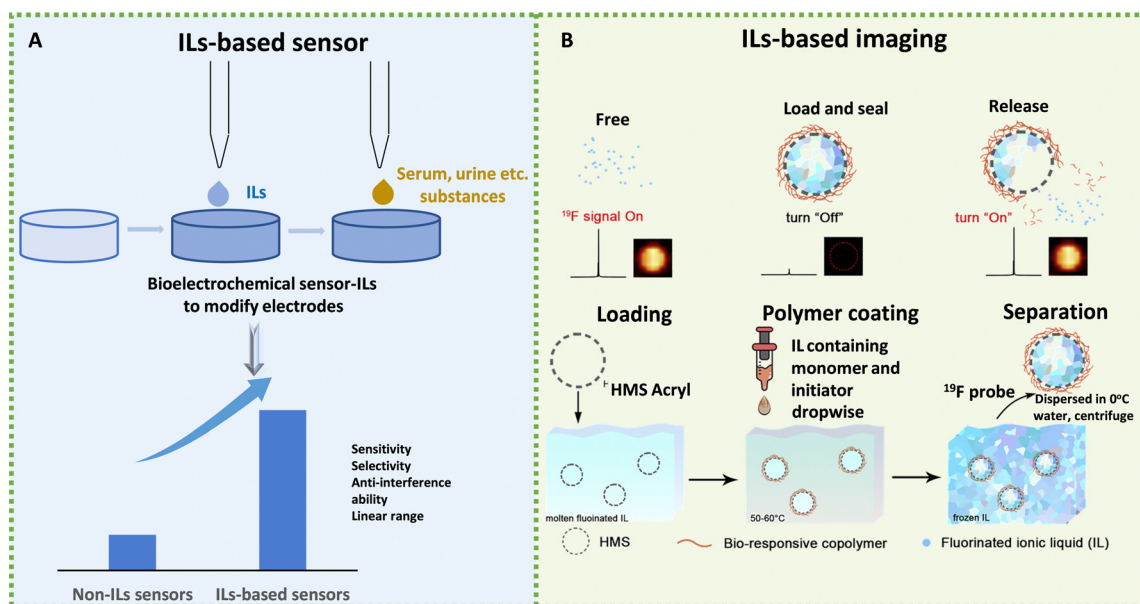


Fig. 7 Schematic diagram of the application of ILs in disease diagnosis. (A) Schematic diagram of IL-based sensors to test substances. (B) Schematic diagram of the <sup>19</sup>F MRI platform for stimuli-responsive <sup>19</sup>F MRI. Reproduced with permission from ref. 210. Copyright 2020 Elsevier.



bromide ([HOOCMIM][Br]) to detect HSA.<sup>211</sup> TPE-IL molecules spontaneously docked with the hydrophobic subdomain of HSA because of the hydrophobic and H-bond interactions between TPE-IL and the amino acid residues of HAS, inducing fluorescence intensity enhancement. This sensor showed good sensitivity, selectivity, anti-interference ability, a linear range of 0.02–10  $\mu\text{g mL}^{-1}$ , and a detection limit of 0.007  $\mu\text{g mL}^{-1}$ , whose practicability was demonstrated by precise detection of HSA levels in human urine and serum samples.<sup>211</sup> Boobphahom *et al.* developed a paper-based sensor decorated with 1-butyl-2,3-dimethylimidazolium tetrafluoroborate ([BdMIM][BF<sub>4</sub>]), CuO, and reduced graphene for the non-enzymatic detection of creatinine. ILs acted as a charge transferring bridge, providing electro-catalytic ability and high ionic conductivity, resulting in an increased electron-transfer rate and a fast signal response. The linear detection range of the sensor was 0.01–2.0 mM with a limit of detection of 0.22 mM (S/N = 3) for creatinine detection.<sup>212</sup> Teekayupak *et al.* fabricated a simple electrochemical sensor for non-enzymatic detection of creatinine, based on 3D-printed electrodes decorated by CuO-[BdMIM][BF<sub>4</sub>]/rGO (reduced graphene oxide).<sup>213</sup> The modified electrodes could directly couple with a portable smartphone potentiostat controlled by an Android app. The linear detection range of the sensor was 0.5–35.0 mM with a limit of detection of 37.3  $\mu\text{M}$ . These IL-based sensors show promise in the early detection and monitoring of kidney diseases.

IL-based sensors could be used to diagnose diabetes because ILs have shown specific achievements in the diagnosis of glucose and acetone, common indicators of diabetes. Graphene is a topical issue in electrochemical sensor research because of its unparalleled 2D honeycomb nanostructures, large specific surface area, as well as strong mechanical properties.<sup>214–216</sup> The interaction between graphene and ILs can occur through electrostatic interaction,  $\pi$ - $\pi$  stacking, H-bonds, and covalent bonds. The common ILs used for modifying graphene involve imidazolium-based ILs, ammonium-based ILs, phosphonium-based ILs, pyridinium-based ILs, and amine-terminated ILs (ILs-NH<sub>2</sub>). For instance, graphene, which contains a large number of  $\pi$  electrons, can interact with imidazole cations that are positively charged. Moreover, the aromatic rings present in imidazole cations can interact with graphene surfaces through  $\pi$ - $\pi$  stacking interactions.<sup>217</sup> ILs-NH<sub>2</sub> can also react with epoxy groups on GO to form covalent bonds.<sup>218</sup> The introduction of ILs not only produces IL-functionalized graphene with excellent conductivity, stability, and dispersibility, but also prevents the aggregation of graphene.<sup>219,220</sup> Luan *et al.* constructed an enzyme-free glucose sensor by mixing Ni<sub>3</sub>S<sub>2</sub> nanomaterials with 1-(3-aminopropyl)-3-methylimidazolium bromide ([A-MIM][Br])-functionalized graphene. This sensor possessed a satisfactory detection range with a wide linear range of 0–500  $\mu\text{M}$ , strong anti-interference ability, excellent sensitivity, and good repeatability. The synergistic effect of electrochemical performance occurred between Ni<sub>3</sub>S<sub>2</sub> and IL-functionalized graphene, which optimized conductivity and made the response more sensitive.<sup>221</sup> Nishan *et al.* developed a colorimetric sensor for acetone detection based on the eosin dye, which reacted with acetone in

the presence of protic IL 1-*H*-3-methylimidazolium ([H-MIM]-[Br])-coated TiO<sub>2</sub> nanoparticles (NPs). The sensor exhibited a wide linear range from  $1.6 \times 10^{-6}$  to  $6.1 \times 10^{-5}$  mol L<sup>-1</sup>, a low limit of detection, only 5 min response time, and good selectivity and sensitivity.

IL-based sensors could be used to diagnose gout as they can enable more sensitive detection of uric acid (UA) in human blood and urine, which is highly beneficial for early disease diagnosis.<sup>222,223</sup> Abbas *et al.* developed an electrochemical sensor for the real-time monitoring of UA using benzimidazolium-1-acetate to modify the electrode, which increased the intrinsic conductivity and thermal stability, due to the availability of high  $\pi$ -electron density from availability of carboxyl functional groups and aromatic rings. The sensor exhibited a highly sensitive and selective response, excellent anti-interference ability, a linear range of 2–1050  $\mu\text{M}$ , as well as a detection limit of 1.27  $\mu\text{M}$ , and was effective in monitoring UA from blood of gout patients and healthy individuals.<sup>224</sup>

IL-based sensors could be used to diagnose cancer and can exploit differences to detect cancer-specific biomolecules. Molecular imprinting is a commonly used technique to create recognition sites in a polymer matrix that are specific to a target molecule. In this context, the polymerized IL hydrogel could act as the matrix and cancer-specific biomolecules could serve as the template molecule for the molecular imprinting process. For instance, Wang *et al.* used polymerized 3-[[[(4-*N,N*-bis-[(carbamoyl)ethylmethacrylate]butyl)((carbamoyl)amino)ethyl methacrylate]-propyl]-1-ethenyl-1imidazol-3-ium bromide ([BCCPEim][Br]) hydrogel as a matrix for the molecular imprinting of the target molecule carcinoembryonic antigen (CEA).<sup>225</sup> The resulting molecularly imprinted polymer was then integrated into a photoelectrochemical sensor for CEA detection. The vinyl, amino and imidazolium cations in the polymerized [BCCPEim][Br] hydrogel interacted with CEA through hydrogen bonding and electrostatic attraction, providing complementary active sites that interact with CEA. The polymerized [BCCPEim][Br] hydrogel might have had a rigidity that helped maintain the structure of CEA and the intermolecular interaction between CEA and the imprinted active site, improving the sensing performance of CEA with high selectivity, sensitivity, and stability. The molecularly imprinted sensor displayed a linear response ranging from 0.05 to 5.0 ng mL<sup>-1</sup> and a detection limit of 11.2 pg mL<sup>-1</sup>.<sup>225</sup> Compared with the clinical application of chemiluminescence immunoassay, the polymerized [BCCPEim][Br] hydrogel-based sensor had excellent accuracy in detection results, with a relative deviation of less than 5%.

In addition, ILs have been utilized in the determination of other indicators, such as adrenaline and glutathione in human urine samples and whole blood.<sup>226–228</sup> As shown in Table 2, ILs have been widely studied in the modification of electrodes as transfer bridges, functional agents, and linkers to improve electrochemical properties, so as to enhance the sensitivity, selectivity, and other properties of sensors and make it possible to diagnose diseases conveniently and accurately. Accurate monitoring of biomarkers in human blood or urine is crucial



Table 2 Application of ILs in the diagnosis of diseases

Substance to be tested	Related disease	ILs	The action of ILs	Linear range	Detection limit	Ref.
HSA	Kidney diseases	[HOOCMIM][Br]	TPE-IL for fluorescence	0.02–10 $\mu\text{g mL}^{-1}$	0.007 $\mu\text{g mL}^{-1}$	211
Creatinine	Kidney disease	[BdMIM][BF <sub>4</sub> ]	Modify electrodes	0.01–2.0 mM	0.22 $\mu\text{M}$	212
Creatinine	Kidney diseases	[BdMIM][BF <sub>4</sub> ]	Modify electrodes	0.5–35.0 mM	37.3 $\mu\text{M}$	213
Glucose	Diabetes	[A-MIM][Br]	Functionalize graphene	0–500 $\mu\text{M}$	0.161 $\mu\text{M}$	221
Acetone	Diabetes	[H-MIM][Br]	Moderator for improved sensing properties of TiO <sub>2</sub>	$1.6 \times 10^{-6}$ – $6.1 \times 10^{-5}$ M	$2.7023 \times 10^{-5}$ mM	229
UA	Gout	BIL	Boost up the intrinsic conductivity and thermal stability of electrodes	2–1050 $\mu\text{M}$	1.27 $\mu\text{M}$	224
Ascorbic acid, DA, and UA	Gout, Parkinson, schizophrenia, etc.	[BMIM][PF <sub>6</sub> ]	Modify electrodes	25–400 $\mu\text{M}$ , 0.2–10 $\mu\text{M}$ , and 0.5–20 $\mu\text{M}$ for ascorbic acid, DA, and UA	6.64 $\mu\text{M}$ , 0.06 $\mu\text{M}$ , and 0.03 $\mu\text{M}$ for ascorbic acid, DA, and UA	230
Guanine and UA	Gout	[BMIM][Cl]	Solvents for cellulose	0.6–620 $\mu\text{M}$ and 0.2–460 $\mu\text{M}$ for UA and guanine	0.077 and 0.144 for UA and guanine	231
HPV16 DNA	HPV16-positive head and neck cancer	[APHimi][Cl]	Functionalize graphene	From 8.5 nM to 10.7 $\mu\text{M}$	1.3 nM	232
CEA	Cancer	[BMIM][PF <sub>6</sub> ]	Functionalize graphene	From 0.001 $\text{fg mL}^{-1}$ to 1 $\text{ng mL}^{-1}$	0.0003 $\text{fg mL}^{-1}$	233
CEA	Cancer	[BCCPEim][Br]	Provide a more favorable environment	0.05–5.0 $\text{ng mL}^{-1}$	11.2 $\text{pg mL}^{-1}$	225
Glutathione	Diabetes and alcoholism, etc.	[BMIM]PF <sub>6</sub>	Modify electrodes	0.1–3.0 $\mu\text{M}$	0.04 $\mu\text{M}$	227
Adrenaline	Parkinson's disease	[dMIM][BF <sub>4</sub> ]	Modify electrodes	0.1–400 $\mu\text{M}$	0.07 $\mu\text{M}$	228
DA and UA	Depression, etc.	[BMIM][Br]	Modify electrodes	0.1 to 300.0 $\mu\text{M}$ for DA	0.04 $\mu\text{M}$ for DA	234
Choline and acetylcholine	AD, Parkinson diseases, etc.	[AMIM][NTF <sub>2</sub> ]	GO-IL to provide a more favorable micro-environment	5–1000 nM for choline and acetylcholine	0.885 and 1.352 nM for choline and acetylcholine	13
O <sub>2</sub> <sup>•-</sup>	AD etc.	IL polymer	Prevent enzyme leakage	1.0–228.0 $\mu\text{M}$	0.42 $\mu\text{M}$	235

not only for early detection, but also for effective treatment of various diseases. However, it would be impossible for most people to go daily to the hospital for physical examination. Therefore, detecting these indicators using a portable and easy to use sensor based on ILs while maintaining accuracy is also an important goal for the development and improvement of sensors.

**4.2.2 IL-based sensors to diagnose mental diseases.** The diagnosis of physical diseases based on ILs is convenient and accurate, while the diagnosis of mental diseases is relatively difficult, which are mainly evaluated through an interview with the patient.<sup>236–238</sup> However, the poor availability of objective methods hampers both diagnosis and treatment for mental diseases. Hence, objective and efficient diagnostic approaches of mental diseases are in great demand. There are substances that can be detected to aid or directly diagnose mental diseases, and ILs can be involved in making sensors to detect these substances.

IL-based sensors have the potential to aid in the diagnosis of depression. ILs can enhance the sensitivity of electrode detection by improving the electron transfer between the electrode surface and target molecules, because of ILs' high conductivity. The low sensitivity of dopamine (DA) detection in the brain, caused by its low concentration, could be effectively improved by the addition of ILs. Nagles *et al.* developed a novel sensor with an electrode modified by chitosan-single walled carbon nanotubes and [BMIM][BF<sub>4</sub>]. The sensitivity of the IL-modified electrodes improved compared with electrodes without IL

modification under the same conditions. Specifically, the anodic peak current of DA detected using [BMIM][BF<sub>4</sub>]-modified electrodes increased by 17%.<sup>239</sup> The neurotransmitter serotonin (5-hydroxytryptamine, 5-HT) played a critical role in the emotional system and the involvement of ILs in 5-HT sensors could aid in the diagnosis of depression. Li *et al.* developed a highly sensitive nanocarbon 1-octylpyridinium hexafluorophosphate paste electrode for the detection of 5-HT. The electrode exhibited a linear range of 0.2–20  $\mu\text{M}$  and a detection limit of 0.1  $\mu\text{M}$ . The addition of highly conductive ILs was found to significantly enhance the electron transfer rate and increase the measured current, leading to improved sensitivity.<sup>240</sup> Yang *et al.* also developed an electrochemical biosensor for the detection of glucocorticoid receptor alpha, a key biomarker of depression in the hippocampus and blood cells. The biosensor utilizing amino acid-coated gold NPs and amino-ion rGO (IL-rGO) markedly magnified the electrochemical signals.<sup>241</sup>

IL-based sensors could be used to diagnose AD. Choline and acetylcholine play crucial roles in various biological processes, for example, cognitive processes.<sup>242,243</sup> Since some diseases are connected with choline and acetylcholine, which were used as biological media, the quantitative analyses of choline and acetylcholine are possibly helpful for diagnosis of AD. In the work of Albishri *et al.* sensitive and selective biosensors, composed of choline oxidase or acetylcholine esterase on glassy carbon electrode decorated GO-1-allyl-3-methylimidazolium bis(trifluoromethylsulfonyl)imide ([AMIM][NTF<sub>2</sub>]), were designed for the determination of choline and acetylcholine in human





serum samples. ILs played an excellent role in the sensor, they could be used as modifiers to improve the performance of electrodes.<sup>244,245</sup> Furthermore, the combination of GO and ILs could provide a more advantageous microenvironment for the stabilization and enhancement of catalytic performance for immobilized enzymes.<sup>13</sup> The quantitative analysis of  $O_2^{\bullet-}$  is important in early diagnosis of AD induced by ROS.<sup>246–249</sup> Peng *et al.* fabricated a carbon fiber microelectrode for acute and sensitive monitoring of  $O_2^{\bullet-}$  in living rat brains. The electrode was coated by a functionalized polymer carboxyl-rich IL onto Prussian blue NPs. Biocompatible polymer ILs prevented enzyme leakage by abundant points with superoxide dismutase, which was beneficial for the improvement of the sensitivity.<sup>235</sup>

ILs show excellent advantages for the production of sensors to diagnose diseases, which are mostly achieved by modifying electrodes. Due to the special structure of ILs, they can form H-bonds with a variety of substances, provide active sites for reactions, and have good electrochemical properties. These advantages enable ILs to modify the surface of a variety of substances to use in disease diagnosis. Currently, the primary approaches of mental disease diagnosis are through interview to identify the signs and symptoms. Therefore, it is crucial to develop IL-based sensors with low detection limits, high accuracy, sensitivity, and selectivity in the diagnosis of mental illnesses.

**4.2.3 ILs in MRI/fluorescence diagnosis.** ILs can play important roles as the element or fluorescence providers in imaging diagnosis. ILs, with their tunable structure and excellent performance, can also contribute to enhance diagnosis in the biomedical field, such as through magnetic resonance imaging (MRI). For example, in comparison with hydrogen nuclear magnetic resonance with its limitations of strong background, low contrast, and imaging artifacts, researchers' attention has been drawn to  $^{19}\text{F}$  MRI, where ILs were recognized as potential candidates of possible fluorinated ions, *i.e.*, [BMIM][BF<sub>4</sub>] and 1-ethyl-3-methylimidazolium trifluoromethyl sulfonate ([EMIM][OTf]).<sup>210,250</sup> There is a great demand for the  $^{19}\text{F}$  agents with superior performance. Zhu *et al.* utilized the phase transition of ILs to contact hollow mesoporous silica (HMS) and stimuli-responsive substances to form a core-shell structure. Fluorinated ILs as cargos were loaded in molten state into carrier HMS and sealed with bio-responsive copolymers, resulting in the formation of “ $^{19}\text{F}$  off” (Fig. 7B). When triggered by bio-stimuli like acid tumor microenvironment or overexpressed MMP, “ $^{19}\text{F}$  on” was lighted up *in vivo*.  $^{19}\text{F}$  MRI was thus considered as a promising platform to diagnose diseases like cancer. These fluorinated IL probes hold many advantages, such as low background value, deep tissue penetration, good biocompatibility and sensitivity, which are beneficial to *in vivo* imaging.<sup>210</sup>

The use of fluorescent ILs probe for real-time monitoring is a novel approach. A fluorescent IL, *N*-methyl-6-hydroxyquinolinium bis(trifluoromethylsulfonyl)imide ([6MQc][NTf<sub>2</sub>]) probe had advantages of high fluorescence sensitivity to pH in the range of 6.0–7.5, selectivity, and biocompatibility for the quantitative imaging of intracellular pH. These were elucidated by

Gao *et al.*, who offered a crucial tool responsible for the early diagnosis of diseases.<sup>251</sup> Dramatic fluctuations in intracellular pH can induce inappropriate cell growth, division, and function, and cause serious diseases.<sup>252–255</sup> Hence, this real-time monitoring of intracellular pH was of significance for disease diagnosis and prevention.

Magnetic ILs composed of imidazolium cations based on perylene diimide (PDI) and anions of nitrate-chelated Gd(III) were established and the Gd(III) complex was used to enhance the MRI signals, while the PDI was applied in fluorescence imaging. The magnetic ILs were dispersed on the membrane in a formation with excellent luminous properties, making them valuable for fluorescence imaging of cells and tissues. In the aqueous environment, the magnetic ILs were aggregated by the  $\pi$ - $\pi$  stacking interaction of cations, facilitating the enhancement of MRI signals on tumor tissues. The switching characteristic between the dispersed and aggregated formation, depending on changes in the physiological environment, makes this magnetic IL suitable for dual-mode imaging through fluorescence imaging and MRI.<sup>256</sup>

The structural tunability of ILs creates many possibilities for composition. ILs can be used as element donors and luminescence factors in imaging diagnosis, suggesting abundant applications in the diagnosis of disease influence. Moreover, the different states of ILs hold promise for imaging diagnosis. For example, the IL contrast agent is wrapped in the molten state, sealed in the solid state, and then followed by surface modification according to the particularity of the micro-environment or surface protein expression of disease lesions to achieve the purpose of targeted release for imaging. IL monomers with aromatic rings can be designed for fluorescence imaging by  $\pi$ - $\pi$  stacking interactions after polymerization or aggregation in the micro-environment of disease foci. Until now, diagnosis and treatment have been mostly separated. ILs with dual characteristics of fluorescence/imaging and treatment can break the routine and combine diagnosis and treatment by introducing the  $^{19}\text{F}$  element into ILs with anti-cancer activity and then wrapping them in a shell that responds to the tumor site or attaching folic acid targeting to tumors. These design tasks can be tedious and complex and can be simplified by using the learning and prediction abilities of AI.

### 4.3 Application of ILs in delivery systems

Controlled drug release systems with enhanced drug efficacy and minimized side effects have garnered significant attention from researchers. To meet this demand, various organic and inorganic systems, such as hydrogels, micelles, and nano-controlled drug release delivery systems, have been developed.<sup>257,258</sup> Considering the tunability of ILs' structure, different response sensitive drug release systems could be designed under various conditions through the selection of compatible cationic and anionic moieties. In this section, we discuss current progress in IL drug delivery.

**4.3.1 Drug assistants.** The amphiphilic nature of ILs, characterized by their ability to dissolve both hydrophilic and hydrophobic compounds, along with the tunability of their



anions and cations, offers great potential for optimizing drug solubility in solution systems. The effectiveness and safety of medicine formulations are key factors reflecting the drug level.<sup>259</sup> However, many drugs suffer from low bioavailability because of insolubility. A solution system based on ILs could dissolve hydrophobic drugs under mild dissolution conditions in a short time, greatly increasing the concentration of drugs in water (Fig. 8A).<sup>8,260</sup> For example, a small amount of choline lysinate ([Ch][Lys]) could significantly increase the solubility of ferulic acid and puerarin, because [Ch][Lys] would improve the solubility of hydrophobic substances.<sup>261</sup> CAGE also improved the bioavailability of sorafenib (a hydrophobic drug) by increasing its solubility through oral delivery. Briefly, CAGE improved

the solubility, increased the concentration in the blood, and extended the release time in the body, thereby improving efficacy.<sup>262</sup>

In addition to increasing solubility, ILs can increase the permeability of drugs.<sup>8</sup> They can be used as chemical permeation enhancers to break down physiological barriers and deliver active ingredients to disease sites.<sup>10</sup> Thus, application of ILs as a delivery system is feasible. Furthermore, combining cations or cations of biologically active pharmaceutical ingredients (APIs) with ILs can form IL-API drugs, which can promote the dissolution of poorly water-soluble drugs as innovative solutions, enabling reaching target cells through various barriers.<sup>265</sup> For example, Lu *et al.* synthesized IL-based taurine

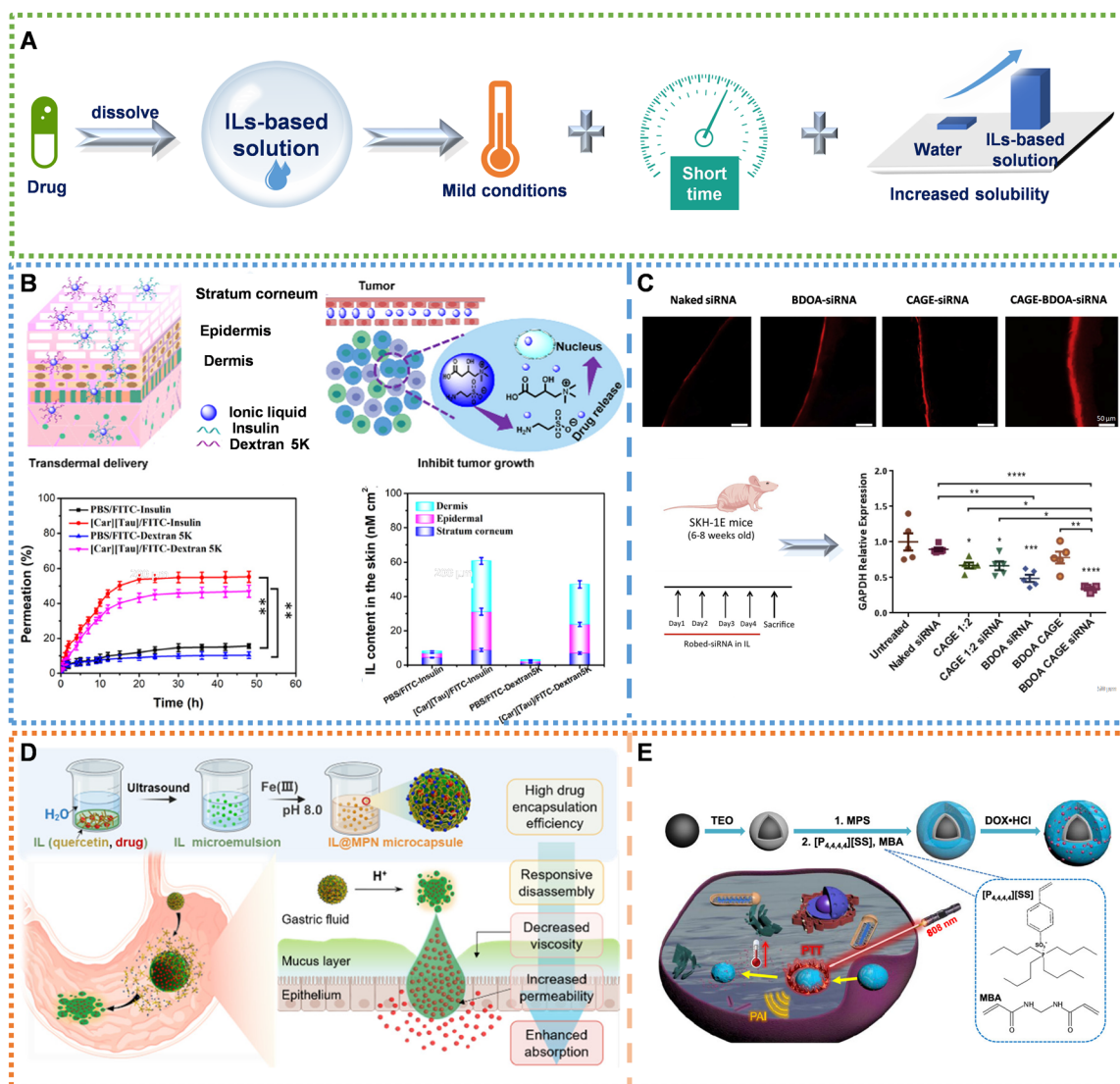


**Fig. 8** Application of ILs in delivery systems. (A) Schematic diagram of ILs increasing drug solubility. (B) Schematic diagram of [Car][Tau] delivering insulin and dextran to tumor cells, inhibition of tumor growth (top), permeation of drugs across the skin with [Car][Tau] (left), and the content of IL delivery drugs in different layers of the skin (right). Reproduced with permission from ref. 263. Copyright 2021 American Chemical Society. (C) Topical delivery of siRNA-ILs through porcine skin *in vitro* (top) and gene knockdown by siRNA-IL formulation correlated with biological efficacy *in vivo* (bottom). Reproduced with permission from ref. 11. Copyright 2020 Elsevier. (D) Preparation of IL-based microemulsion and the proposed oral drug delivery system. Reproduced with permission from ref. 264. Copyright 2022 American Chemical Society. (E) Poly[P4,4,4,4][SS] as the pH- and thermally responsive receiver coated with CuCo<sub>2</sub>S<sub>4</sub> nanoparticles to deliver drugs. Reproduced with permission from ref. 21. Copyright 2020 American Chemical Society.



with good biocompatibility, non-toxicity, and antitumor activity to deliver insulin and dextran.<sup>263</sup> The results showed that taurine-based ILs could improve the drug permeability and efficacy (Fig. 8B).<sup>263</sup> A biocompatible IL choline fatty acid [Ch][FA] was used as a skin permeation enhancer to mediate the dissolution of antigen peptides to treat tumor. Compared with the use of water solvent, the transdermal delivery flux of peptides increased 28-fold by using the IL. Furthermore, no skin irritation was caused and tumor growth *in vivo* was successfully inhibited.<sup>266</sup>

Mitragotri's team has been committed to the exploration of ILs in the field of biomedicine and made great advancements in using ILs as drug permeation enhancers in recent years. They presented siRNA robed with IL moiety (benzyl dimethyl octyl ammonium (BDOA)-siRNA) for the treatment of skin disease. The system displayed the necessary properties for dermal drug delivery, including biocompatibility, cell internalization, and skin permeability irrespective of the siRNA. The experiments demonstrated that therapeutic BDOA-siRNA could be viewed as a promising prodrug platform for treating skin diseases such as psoriasis, atopic dermatitis, and melasma.<sup>267</sup> They developed complementary and synergistic strategies to deliver siRNA into the skin for a topical therapeutic administration (Fig. 8C).<sup>11</sup> Demonstrating that BDOA-siRNA effectively permeated the labeled siRNA into the epidermis *in vitro* using the CAGE system for topical delivery. Furthermore, the administration of CAGE-BDOA siRNA to SKH1-E hairless mice resulted in a significant reduction of 44% in the expression of GAPDH protein compared with the group treated with CAGE-BDOA alone. This reduction was also 13-fold greater compared with the untreated group.<sup>11</sup>

ILs can effectively improve the water solubility of insoluble drugs and the permeability of drugs. They can promote absorption, break the physiological barrier, and improve drug bioavailability because of miscibility and ability to disrupt the lipid bilayer structure of biological membranes. However, the use of ILs as solution and permeation enhancers can have adverse effects, such as causing irritation or damage to the mucosal barriers or skin. Thus, ILs must be reasonably designed, and careful selection of their concentrations is needed to ensure the safety and efficacy of IL-based drug delivery systems.

**4.3.2 Vaccine adjuvants.** Adjuvants, which are non-specific immunoenhancers, are crucial for enhancing the immunogenicity of antigens. Currently, inorganic salt adjuvants, oil emulsion adjuvants, bacterial lipids, and foreign genomic substances are the main types of adjuvants used. However, they are associated with safety concerns, poor stability, and ineffective immune activation.<sup>268</sup> ILs have emerged as a promising alternative to traditional adjuvants because of their biocompatibility, stability, and controlled release, all of which enhance their effectiveness as adjuvants. Furthermore, ILs are effective adjuvants because they can activate immune cells and modulate the immune response.

ILs with good biocompatibility (*e.g.*, based on original human metabolites) have been explored for the development of vaccine adjuvants. For example, choline dihydrogen

phosphate IL has been used to enhance the therapeutic merit of vaccine candidate KMP-11 (a small protein) towards leishmaniasis under parenteral injection.<sup>269</sup> Pancreatic ductal adenocarcinoma cells treated with CAGE enhanced immunogenicity and permeability of tumor cells.<sup>270</sup> Mitragotri's team developed a new IL adjuvant synthesized using choline and lactic acid. It had good biocompatibility and a dispersion effect on ovalbumin antigen, induced effective antigen-presenting cell infiltration at the injection site, and generated a strong immune response to antigen.<sup>271</sup> Zhang and colleagues were the first to develop an intranasal vaccine adjuvant system for influenza split virus antigen in the form of an oil-in-[Ch][Nic] nanoemulsion formulation with uniform size and excellent stability. This system promoted a robust mucosal immune response in the body, prolonged the nasal residence time (24-fold greater than in control participants), and enhanced the penetration of antigens into the nasal mucosal epithelial cells.<sup>272</sup>

At present, ILs used in research as vaccine adjuvants are generally limited to human metabolites. The application of biocompatible ILs in vaccine adjuvants could be expanded. The use of IL adjuvants through different vaccine delivery methods could be developed further. For example, oral vaccine adjuvants must overcome the adverse gastrointestinal tract environment with its strong acidity and digestive enzymes. Sufficient residence time in the gastrointestinal tract is needed for vaccine absorption to ensure that the vaccine can reach the induction site of mucosa-associated lymphoid tissue and trigger the immune response.<sup>273</sup> The diversity of IL structures means that ILs can be designed to have acid resistance and sufficient retention time in the gastrointestinal tract based on the actual requirements of oral vaccine adjuvants.

**4.3.3 Environmental response therapy.** ILs are susceptible to microwave radiation, because of their ionic characteristics and high polarizability and are often used to enhance microwave thermal therapy. Su *et al.* loaded [BMIM][PF<sub>6</sub>] onto nanocomposites for enhancing microwave thermal therapy (MWTT).<sup>274</sup> Chen *et al.* loaded ILs onto ZrO<sub>2</sub> with triphenylphosphonium, a mitochondrial-targeting molecule, and the tumor cell-targeting peptide iRGD to obtain a nano-agent for efficient cancer therapy by microwave ablation.<sup>275</sup> Wu *et al.* loaded ILs as an microwave heating sensitizer and a liquid metal onto mesoporous ZrO<sub>2</sub> nanoparticles to design the first dual-functional nanoparticles with microwave dynamic therapy and microwave thermal therapy by using MW as the sole energy source,<sup>276</sup> synthesizing highly effective anti-tumor drugs. The drugs had CT imaging capability to visually monitor the therapeutic results in real time. Under combination therapy, the tumor inhibition rate of subcutaneous tumor model mice could reach 92.2% ± 6.8% and 40% of the tumor-bearing orthotopic HCC mouse models could be completely cured.<sup>276</sup>

ILs can form pH- or temperature-responsive drug delivery systems with nanoparticles. The hydrophobic alkyl chain and the hydroxyl group of the choline cation in choline acetate could establish a 3D network structure with the polymer chain of P123 through H-bonds and hydrophobic interactions. This





would serve as a potential temperature-responsive drug carrier, allowing the drug to be transported in the gel network.<sup>277</sup> The pH-sensitive microencapsulation, which consists of an IL core and a metal-phenolic network shell, has been proved to be effective for oral drug delivery. ILs effectively loaded drugs and increased the drug transport rate in endothelial cells to improve drug permeability (Fig. 8D).<sup>264</sup> Zhou *et al.* used poly(lactide-*co*-glycolide) as the backbone, choline arginine for protein protection, and vitamin B12-chitosan for mucosal adhesion and pH responsiveness.<sup>278</sup> Choline arginine proved effective in maintaining insulin stability throughout delivery system preparation, transportation, and storage.

ILs can modify nanoparticles to form a multi-stimuli-responsive delivery system. IL-based hydrogels loaded with Fe<sub>3</sub>O<sub>4</sub> nanoparticles could deliver drugs efficiently with corresponding stimulation (pH and temperature), excellent biocompatibility, and self-healing properties.<sup>277</sup> Fan *et al.* proposed a new drug release, which was composed of CuCo<sub>2</sub>S<sub>4</sub> nanoparticles as the core and poly(tetrabutylphosphonium styrene-sulfonate) (Poly[P<sub>4,4,4,4</sub>][SS]) as the pH- and thermally responsive receiver. The results showed that the combinatorial dual stimuli-triggered drug release behaviors can efficiently improve the cytotoxicity of cancer cells (Fig. 8E).<sup>21</sup> Zhou *et al.* developed prochloraz IL-based microcapsules of pesticides.<sup>279</sup> The prochloraz IL was used as nucleating agent to load CaCO<sub>3</sub> onto the surface of micelles and wrap it with pectin. These IL-based microcapsules were pH/pectinase-responsive with excellent antibacterial performance and long-term efficacy against sclerotinia. Yu *et al.* used core-shell liquid-metal nanoparticles modified with 1-butyl-3-methylimidazolium (*L*)-lactate to combine chemodynamic therapy (CDT), microwave dynamic therapy (MDT), and MWTT.<sup>280</sup>

IL complexes, which are a class of ionic polymers can often bind responsive groups such as photo-, pH-, and thermally responsive groups. Cui *et al.* exploited microenvironmental changes in tumor cells to fabricate self-assembled nanoparticles with thermal and pH responses.<sup>281</sup> Poly(IL-*co*-*N*-isopropylacrylamide) (PILNPM20) combined with deoxycholic acid was pH and thermal dual-responsive. PILNPM20 based on IL complexes was the polyelectrolyte backbone. The self-assembled nanoparticles can be used as drug carriers to effectively control drug release. An amphiphilic block polymer containing an IL complex, consisting of three parts: a target ligand, photo-response block, and pH-response block, could self-assemble into drug-loaded nanoparticles with a particle size of 80 nm in aqueous solutions, and the drug loading capacity of doxorubicin (DOX) was as high as 70%.<sup>282</sup> Nanoparticle based IL complexes had no obvious side effects and good biocompatibility.

IL-response sensitizers are used as drug release switches and carriers for specific functions in biomedicine to maximize the effects. The relationship between nanoparticles and the environment can be reconciled by selecting appropriate ILs to modify the surface of nanoparticles. ILs provide new directions for nanomaterials and as pharmaceutical preparations, to treat diseases. However, the combination of nanomaterials and ILs

requires comprehensive evaluation, including internal stability *in vivo*, biological distribution, and metabolic pathways, to assess drug safety and long-term biological behavior *in vivo*. At the same time, ILs often modify the surface of nanomaterials, which limits drug loading. Therefore, surface modification and drug activity should be balanced.

**4.3.4 Drug carriers.** ILs have been demonstrated to increase the solubility and bioavailability of drugs. Additionally, they can be designed to exhibit controlled release properties that are advantageous in maintaining drug concentrations at therapeutic levels for an extended duration. Mitragotri *et al.* found that choline-geranate-based IL (LATTE) could be used as a drug carrier and ablation agent for percutaneous locoregional therapies of hepatocellular carcinoma.<sup>283</sup> A single LATTE injection led to uniform distribution and retention of drugs in the ablation area for up to 28 days, helping in prevention of tumor recurrence. LATTE facilitated the internalization of DOX and exhibited great potential to kill cancer cells when used in combination, compared with individual DOX usage. Additionally, LATTE treatment led to a rapid and substantial reduction of adenosine triphosphate (ATP), which could prevent cancer cells from converting glycolytic ATP to induce resistance.<sup>283</sup> LATTE might promote a microenvironment conducive to immunotherapy in animal models based on histological analysis.

ILs have the unique ability to self-assemble into nanostructures in solutions. They can form different structures (introduced in Section 2.2), such as micelles, vesicles, and microemulsions. The diversity of IL structures also provides a broader space to increase drug solvation as drug carriers. IL-based drug carriers have good stability.<sup>284</sup> They can change their structure by adjusting pH, temperature, light, enzyme and other physical or chemical stimuli for drug release. After receiving external stimulation, the structures of the carriers are often destroyed and the hydrophilicity or hydrophobicity changed, resulting in drug carriers becoming loose or shrinking to achieve the purpose of drug release. CAGE was combined with Tween 20 to form a microemulsion in water and loaded with methotrexate (MTX) for the treatment of psoriasis.<sup>285</sup> The IL-based drug carrier system was thermo-responsive for release of MTX. When the temperature changed, the carrier transformed from a hydrophilic state to a hydrophobic state, leading to the contraction of the hydrogel network and the release of drugs. Further experiments on mice have proved excellent ability to deliver MTX through the skin, which could effectively treat skin inflammation without adverse side effects.

PILs have also made significant progress as drug carriers. PILs usually exhibit lower biological toxicity than IL monomers. Stimulation-responsive PILs have a wide range of applications and widely researched as drug carriers, suggesting that they are expected to become candidates for drug delivery. For example, 1-vinyl-3-butylimidazolium bromide ([VBIM][Br]) monomers were polymerized into hydrogels to coat the hydrophilic antibacterial drug tetracycline, and the ordered hydrogel molecular chains were disrupted into disordered molecular chains by temperature induction to release drugs.<sup>286</sup> The drug release rate and cumulative release amount in this PIL-based hydrogel



were profoundly biocompatible *in vitro* and could be precisely controlled by adjusting the temperature. Mukesh *et al.* reported a nanogel system, composed of choline acrylate-based PIL, which was able to release up to about 80% 5-fluorouracil, widely used in the treatment of cancer, at pH 1.2 (stomach pH) for 10 days at physiological human body temperature (37 °C). The system had a poor performance at pH 5.0 and 7.4.<sup>287</sup>

Apart from the aforementioned merits, ILs also can redirect the biodistribution and prolong their circulation by modifying the behavior of drug carriers. For example, Hamadani *et al.* developed a protein-avoidant IL strategy to modify nanoparticles for increasing bloodstream circulation and driving biodistribution.<sup>288,289</sup> Compared with PEG modification with the risk of developing anti-PEG antibodies, the introduction of an IL (choline hexenoate) endowed the nanoparticles with negative charge and a larger hydrodynamic radius, resulting in diminished protein adsorption and reduced liver biodistribution.<sup>288</sup> In addition, choline hexenoate could also be used to electrostatically solvate copolymers by direct dissolution, form stable drug carriers, reduce hemolysis, and imbue the ability of hitchhiking onto red blood cells.<sup>62</sup> Furthermore, a library of choline carboxylate ILs assembled on polymeric nanoparticles was constructed to break biological barriers and prolong drug circulation for intravenous delivery.<sup>290</sup> These findings and protocols highlighted the potential of ILs for advanced nanoparticle modification toward the development of more effective and precisely targeted therapies.

ILs have gained attention in drug delivery systems due to their ability to dissolve poorly soluble drugs and regulate the physiological properties of active drug ingredients. Challenges such as poor drug solubility, systemic toxicity, and short retention time remain significant hurdles in the field of biomedicine. The design of high drug-loading and stable supports based on ILs, by combining the diversity of IL cluster forms, is of great practical significance for the effective treatment of drugs with low bioavailability. The form of ILs plays a crucial role in their suitability for drug delivery applications. While there have been advancements in the investigation of IL clusters, more powerful and systematic research on their formation, morphology, and properties is needed to be explored. Additionally, a more thorough understanding of the transport principles governing the use of IL-based delivery systems in cellular uptake and tissue delivery is needed to be elucidated.

## 5 Conclusions and outlook

ILs offer remarkable advantages in biomedical development owing to their unique structures and biological and physicochemical properties. This review provides a detailed overview of the molecular composition, interaction forces of ILs, and the unique physicochemical properties, especially the ILs' tertiary structures (from molecular structure, to H-bonding networks, and to clusters). Furthermore, the therapeutic potential of ILs and their interaction with cell structures are described, along with the underlying mechanisms. This review also highlights

the potential applications of ILs in pharmaceutical engineering, disease diagnosis, and drug delivery systems, taking into account ILs' unique tertiary structures or other tunable physicochemical properties.

ILs have been used in many biomedical fields, yet there are still challenges to be addressed. Firstly, safety remains a significant challenge. Although approved drugs can be ionized into ILs, effectively improving their solubility and bioavailability, the efficacy and dosage still require further exploration. Second, the potential mechanism of ILs as biomedicine needs to be further elucidated *in vitro*. Several indications (*e.g.*, side chain effect) have been identified, but they are insufficient to guide the design of biomedical ILs. Third, regarding the simple biological evaluation system of ILs *in vivo*, it is necessary to expand experimental animal models (beagles and other large animals) to establish a multi-level and full chain biological evaluation system for the safety of ILs. Fourth, the exploration of IL clusters has been insufficient to date. Their formulation, morphology, and properties should be explored using more powerful and systematic methodologies, given the rapid development of IL clusters for the application of drug delivery. Ultimately, more attention should be directed to addressing the residual ILs in the post-treatment processes of pharmaceutical engineering. Meanwhile, it is crucial to emphasize the impact of residual ILs on drug efficacy.

Based on the above discussions, ILs have potential to significantly impact the expansion of multiple drug formulations and routes of administration. Firstly, ILs can serve as protective additives and therapeutic drugs. For example, ILs have shown impressive inhibitory effects on pathogenic bacteria. Therefore, they have the potential to become protective additives to be added in clothing, masks, hand sanitizers, *etc.* Moreover, based on the side chain effect of ILs to break cell membranes, ILs might be used in antiviral activity against enveloped viruses, such as human immunodeficiency virus (HIV), Epstein–Barr virus (EBV), and severe acute respiratory syndrome coronavirus 2 (SARS-CoV-2). By leveraging the membrane-breaking effect of ILs, they might have the potential to inhibit the replication or entry of these enveloped viruses, contributing to the development of effective antiviral strategies. Secondly, utilizing AI to design IL drugs by incorporating parameters such as IL structures and therapeutic effectiveness results in a new shortened drug development time. Thirdly, ILs are potential biomedical aids for synthetic biology regarding the improvement of enzyme stabilization and activity, making them useful for biocatalytic reactions. ILs can also serve as efficient reaction media for critical processes like recombinant DNA and modular enzyme assembly. Fourthly, their miscibility, designability, and tertiary structures, especially clusters, make ILs attractive for drug delivery applications. Overall, the application of ILs in biomedicine is vast and seems borderless.

## List of abbreviations

### Cations

[EMIM]	1-Ethyl-3-methylimidazolium
[BMIM]	1-Butyl-3-methylimidazolium



[HMIM]	1-Hexyl-3-methylimidazolium
[OMIM]	1-Octyl-3-methylimidazolium
[C <sub>10</sub> MIM]	1-Decyl-3-methylimidazolium
[C <sub>12</sub> MIM]	1-Dodecyl-3-methylimidazolium
[C <sub>14</sub> MIM]	1-Tetradecyl-3-methylimidazolium
[C <sub>16</sub> MIM]	1-Hexadecyl-3-methylimidazolium
[HOC <sub>n</sub> C <sub>m</sub> OHL <sub>m</sub> ]	(1-( <i>n</i> -Hydroxyalkyl)-3-( <i>n</i> -hydroxyalkyl)imidazolium
[A-MIM]	1-(3-Aminopropyl)-3-methylimidazolium
[APHimi]	3-(2-Aminoethyl)-1-propyl-1 <i>H</i> -imidazol-3-ium
[BdMIM]	1-Butyl-2,3-dimethylimidazolium
[dMIM]	1,3-Dipropylimidazolium
[H-MIM]	1- <i>H</i> -3-methylimidazolium
[Ch]	Choline
[C <sub>2</sub> NH <sub>2</sub> MIm]	1-Aminoethyl-3-methylimidazolium
[MOEMIm]	1-Methoxyethyl-3-methylimidazolium
[HOEMIm]	1-Hydroxyethyl-3-methylimidazolium
[6MQc]	<i>N</i> -Methyl-6-hydroxyquinolinium
[TBP]	Tetrabutylphosphonium
[PheEt]	<i>l</i> -Phenylalanine ethyl ester
[BCCPEim]	3-(((4- <i>N,N</i> -bis[(carbamoyl)ethyl methacrylate]butyl)((carbamoyl)amino)ethyl methacrylate)-propyl]-1-ethenyl-1 <i>H</i> -imidazol-3-ium
[C <sub>n</sub> C <sub>8</sub> IM]	1-Alkyl-3-octylimidazolium
[Trps]	<i>N</i> -(3-Propanesulfonic acid) tropine
[MerDABCO-SO <sub>3</sub> H]	1,4-Diazabicyclo[2.2.2]octane-4,sulfonic acid
[HOOCMIM]	1-Carboxymethyl-3-methyl-imidazolium
[P <sub>4,4,4,4</sub> ]	Tetrabutylphosphonium
[VBIM]	1-Vinyl-3-butylimidazolium

### Anions

[BF <sub>4</sub> ]	Tetrafluoroborate
[Cl]	Chloride
[Ac]	Acetyl
[Br]	Bromide
[PF <sub>6</sub> ]	Hexafluorophosphate
[SbF <sub>6</sub> ]	Hexafluoroantimonate
[(CF <sub>3</sub> SO <sub>2</sub> ) <sub>2</sub> N]	Bis(trifluoromethyl)sulfonylamide
[ClO <sub>4</sub> ]	Perchlorate
[CF <sub>3</sub> SO <sub>3</sub> ]	Trifluoromethanesulfonates
[NO <sub>3</sub> ]	Nitrate
[CF <sub>3</sub> CO <sub>2</sub> ]	Trifluoroacetate
[1,2,3-Ben]	1,2,3-Benzotriazole
[NTf <sub>2</sub> ]	Bis(trifluoromethanesulfonyl)imide
[Caf]	Caffeate
[Gal]	Gallate
[Ell]	Ellagate
[lys]	Lysinate
[OTf]	Trifluoromethyl sulfonate
[OAc]	Acetate
[FeCl <sub>4</sub> ]	Tetrachloroferrate
[OTs]	<i>p</i> -toluenesulfonic acid
[DHP]	Dihydrogen phosphate

[I]	Iodide
[Bit]	Bitartrate
[Dhc]	Dihydrogen citrate
[SS]	Styrene sulfonate
[MTX]	Methotrexate
[Nic]	Nicotinic acid
[DC]	Deoxycholate
[Doc]	Deoxycholate
[Sar]	Lauryl sarcosinate
[FAs]	Fatty acids

## Conflicts of interest

There are no conflicts of interest to declare.

## Acknowledgements

This work was supported by the National Natural Science Foundation of China (21978292, 21821005, T2225021, and 82341045), the Major Program of National Natural Science Foundation of China (21890762), the International Partnership Program of Chinese Academy of Sciences (Grant No. 122111KYSB20190060), IPE Project for Frontier Basic Research (Grant No. QYJC-2022-012), and National Major Scientific Instruments and Equipments Development Project of National Natural Science Foundation of China (22227811).

## References

- 1 K. S. Egorova, E. G. Gordeev and V. P. Ananikov, *Chem. Rev.*, 2017, **117**, 7132–7189.
- 2 Y. Wang, H. He, C. Wang, Y. Lu, K. Dong, F. Huo and S. Zhang, *JACS Au*, 2022, **2**, 543–561.
- 3 John S. Wilkes and M. J. Zaworotko, *J. Chem. Soc., Chem. Commun.*, 1992, **13**, 965–967.
- 4 P. Dominguez de Maria and Z. Maugeri, *Curr. Opin. Chem. Biol.*, 2011, **15**, 220–225.
- 5 J. Pernak, J. Kalewska, H. Ksycin'ska and J. Cybulski, *Eur. J. Med. Chem.*, 2001, **36**, 899–907.
- 6 I. M. Marrucho, L. C. Branco and L. P. Rebelo, *Annu. Rev. Chem. Biomol. Eng.*, 2014, **5**, 527–546.
- 7 A. R. P. Goncalves, X. Paredes, A. F. Cristino, F. J. V. Santos and C. Queiros, *Int. J. Mol. Sci.*, 2021, **22**, 5612.
- 8 C. Liu, B. Chen, W. Shi, W. Huang and H. Qian, *Mol. Pharmaceutics*, 2022, **19**, 1033–1046.
- 9 X. Lin, Y. Yang, S. Li, Z. Li, Y. Sheng, Z. Su and S. Zhang, *Int. J. Pharm.*, 2022, **625**, 122083.
- 10 Z. Sidat, T. Marimuthu, P. Kumar, L. C. du Toit, P. P. D. Kondiah, Y. E. Choonara and V. Pillay, *Pharmaceutics*, 2019, **11**, 96.
- 11 V. Dharamdasani, A. Mandal, Q. M. Qi, I. Suzuki, M. Bentley and S. Mitragotri, *J. Controlled Release*, 2020, **323**, 475–482.





- 12 R. M. Meira, D. M. Correia, S. Ribeiro, P. Costa, A. C. Gomes, F. M. Gama, S. Lanceros-Méndez and C. Ribeiro, *ACS Appl. Polym. Mater.*, 2019, **1**, 2649–2658.
- 13 H. M. Albishri and D. Abd El-Hady, *Talanta*, 2019, **200**, 107–114.
- 14 V. A. Azov, K. S. Egorova, M. M. Seitkalieva, A. S. Kashin and V. P. Ananikov, *Chem. Soc. Rev.*, 2018, **47**, 1250–1284.
- 15 J. M. Gomes, S. S. Silva and R. L. Reis, *Chem. Soc. Rev.*, 2019, **48**, 4317–4335.
- 16 J. D. Holbrey and K. R. Seddon, *Clean Products and Processes*, 1999, **1**, 223–236.
- 17 S. J. Zeng, X. P. Zhang, L. Bai, X. C. Zhang, H. Wang, J. J. Wang, D. Bao, M. D. Li, X. Y. Liu and S. J. Zhang, *Chem. Rev.*, 2017, **117**, 9625–9673.
- 18 J. Neumann, R. Ludwig and D. Paschek, *J. Phys. Chem. B*, 2021, **125**, 5132–5144.
- 19 B. Yang, L. Bai, T. Li, L. Deng, L. Liu, S. Zeng, J. Han and X. Zhang, *J. Membr. Sci.*, 2021, **628**, 119264.
- 20 K. Wieszczycka, K. Filipowiak, I. Wojciechowska, T. Buchwald, K. Siwińska-Ciesielczyk, B. Strzemiecka, T. Jesionowski and A. Voelkel, *Sep. Purif. Technol.*, 2021, **265**, 118483.
- 21 S. Y. Fan, Y. N. Hao, W. X. Zhang, A. Kapasi, Y. Shu, J. H. Wang and W. Chen, *ACS Appl. Mater. Interfaces*, 2020, **12**, 9000–9007.
- 22 H. Li, T. Niemann, R. Ludwig and R. Atkin, *J. Phys. Chem. Lett.*, 2020, **11**, 3905–3910.
- 23 K. Dong, Y. T. Song, X. M. Liu, W. G. Cheng, X. Q. Yao and S. J. Zhang, *J. Phys. Chem. B*, 2012, **116**, 1007–1017.
- 24 E. Arunan, G. R. Desiraju, R. A. Klein, J. Sadlej, S. Scheiner, I. Alkorta, D. C. Clary, R. H. Crabtree, J. J. Dannenberg, P. Hobza, H. G. Kjaergaard, A. C. Legon, B. Mennucci and D. J. Nesbitt, *Pure Appl. Chem.*, 2011, **83**, 1637–1641.
- 25 H. Y. He, H. Chen, Y. Z. Zheng, S. J. Zhang and Z. W. Yu, *Chem. Eng. Sci.*, 2015, **121**, 169–179.
- 26 A. Karton, M. Brunner, M. J. Howard, G. G. Warr and R. Atkin, *ACS Sustainable Chem. Eng.*, 2018, **6**, 4115–4121.
- 27 K. Dong and S. J. Zhang, *Chemistry*, 2012, **18**, 2748–2761.
- 28 J. M. Vicent-Luna, D. Dubbeldam, P. Gomez-Alvarez and S. Calero, *ChemPhysChem*, 2016, **17**, 380–386.
- 29 L. Cammarata, S. G. Kazarian, P. A. Salter and T. Welton, *Phys. Chem. Chem. Phys.*, 2001, **3**, 5192–5200.
- 30 J. Zhou, X. M. Liu, S. J. Zhang, X. P. Zhang and G. R. Yu, *AIChE J.*, 2017, **63**, 2248–2256.
- 31 A. M. de Ferro, P. M. Reis, M. R. C. Soromenho, C. E. S. Bernardes, K. Shimizu, A. A. Freitas, J. Esperanca, J. N. Canongia Lopes and L. P. N. Rebelo, *Phys. Chem. Chem. Phys.*, 2018, **20**, 19307–19313.
- 32 J. Dupont, *Acc. Chem. Res.*, 2011, **44**, 1223–1231.
- 33 S. M. Chen, S. J. Zhang, X. M. Liu, J. Q. Wang, J. J. Wang, K. Dong, J. Sun and B. H. Xu, *Phys. Chem. Chem. Phys.*, 2014, **16**, 5893–5906.
- 34 L. Shi, F. Chen, N. Sun and L. Zheng, *Soft Matter*, 2015, **11**, 4075–4080.
- 35 H. Y. Wang, L. M. Zhang, J. J. Wang, Z. Y. Li and S. J. Zhang, *Chem. Commun.*, 2013, **49**, 5222–5224.
- 36 M. K. Ali, R. M. Moshikur, R. Wakabayashi, M. Moniruzzaman and M. Goto, *ACS Appl. Mater. Interfaces*, 2021, **13**, 19745–19755.
- 37 I. S. I. Al-Adham, N. Jaber, M. Al-Remawi, F. Al-Akayleh, E. Al-Kaissi, A. S. A. Ali Agha, L. B. Fitzsimmons and P. J. Collier, *Lett. Appl. Microbiol.*, 2022, **75**, 537–547.
- 38 S. P. Callender, J. A. Mathews, K. Kobernyk and S. D. Wettig, *Int. J. Pharm.*, 2017, **526**, 425–442.
- 39 A. R. Bhat, F. A. Wani, K. Behera, A. B. Khan and R. Patel, *Colloids Surf., A*, 2022, **645**, 128846.
- 40 H. Wang, B. Tan, J. Wang, Z. Li and S. Zhang, *Langmuir*, 2014, **30**, 3971–3978.
- 41 S. Shi, T. Yin, X. Tao and W. Shen, *RSC Adv.*, 2015, **5**, 75806–75809.
- 42 X. Li, Y. Guo, H. Wang, Z. Li and J. Wang, *J. Mol. Liq.*, 2022, **352**, 118699.
- 43 X. M. Liu, G. H. Zhou, F. Huo, J. J. Wang and S. J. Zhang, *J. Phys. Chem. C*, 2015, **120**, 659–667.
- 44 G. Singh, K. M. Singh, O. Singh and T. S. Kang, *J. Phys. Chem. B*, 2018, **122**, 12227–12239.
- 45 A. Chandrakar and B. L. Bhargava, *J. Mol. Graphics Modell.*, 2020, **101**, 107721.
- 46 Y. Wang and G. A. Voth, *J. Am. Chem. Soc.*, 2005, **127**, 12192–12193.
- 47 S. S. Urikhinbam and L. S. Shagolsem, *Mater. Today: Proc.*, 2021, **46**, 7044–7048.
- 48 A. M. Curreri, S. Mitragotri and E. E. L. Tanner, *Adv. Sci.*, 2021, **8**, e2004819.
- 49 L. Lomba, A. Polo, J. Alejandre, N. Martínez and B. Giner, *J. Drug Delivery Sci. Technol.*, 2023, **79**, 104010.
- 50 X. Wu, Q. Zhu, Z. Chen, W. Wu, Y. Lu and J. Qi, *J. Controlled Release*, 2021, **338**, 268–283.
- 51 O. Stolarska, A. Pawlowska-Zygarowicz, H. Rodríguez, E. Frydrych-Tomczak and M. Smiglak, *J. Mol. Liq.*, 2021, **339**, 116805.
- 52 A. Boruń, *J. Mol. Liq.*, 2019, **276**, 214–224.
- 53 R. Jain, N. Jadon and K. Singh, *J. Electrochem. Soc.*, 2015, **163**, H159–H170.
- 54 K. Dong, X. Liu, H. Dong, X. Zhang and S. Zhang, *Chem. Rev.*, 2017, **117**, 6636–6695.
- 55 H. Tokuda, K. Ishii, M. A. B. H. Susan, S. Tsuzuki, K. Hayamizu and M. Watanabe, *J. Phys. Chem. B*, 2006, **110**, 2833–2839.
- 56 M. Ahmed, S. S. Rao, A. Filippov, P. Johansson and F. U. Shah, *Phys. Chem. Chem. Phys.*, 2023, **25**, 3502–3512.
- 57 M. Armand, P. Johansson, M. Bukowska, P. Szczeciński, L. Niedzicki, M. Marcinek, M. Dranka, J. Zachara, G. Żukowska, M. Marczewski, G. Schmidt and W. Wieczorek, *J. Electrochem. Soc.*, 2020, **167**, 070562.
- 58 Y. Kohno and H. Ohno, *Phys. Chem. Chem. Phys.*, 2012, **14**, 5063–5070.
- 59 A. A. Freitas, K. Shimizu and J. N. Canongia Lopes, *J. Mol. Liq.*, 2020, **301**, 112402.
- 60 X. Peng, X. Sui, J. Li, T. Liu and L. Yang, *Ind. Crops Prod.*, 2021, **168**, 113596.



- 61 S. Uddin, M. R. Chowdhury, R. Wakabayashi, N. Kamiya, M. Moniruzzaman and M. Goto, *Chem. Commun.*, 2020, **56**, 13756–13759.
- 62 C. M. Hamadani, I. Chandrasiri, M. L. Yaddehige, G. S. Dasanayake, I. Owolabi, A. Flynt, M. Hossain, L. Liberman, T. P. Lodge, T. A. Werfel, D. L. Watkins and E. E. L. Tanner, *Nanoscale*, 2022, **14**, 6021–6036.
- 63 M. R. Chowdhury, R. M. Moshikur, R. Wakabayashi, M. Moniruzzaman and M. Goto, *Int. J. Pharm.*, 2021, **601**, 120582.
- 64 E. Judy and N. Kishore, *Biochimie*, 2022, **207**, 20–32.
- 65 R. Y. Wan, X. H. Xia, P. J. Wang, W. R. Huo, H. Dong and Z. J. Chang, *Toxicol. In Vitro*, 2018, **52**, 1–7.
- 66 P. Bansode, P. Patil, P. Choudhari, M. Bhatia, A. Birajdar, I. Somasundaram and G. Rashinkar, *J. Mol. Liq.*, 2019, **290**, 111182.
- 67 X. Yang, Q. Y. Chen, M. Y. Kong, L. L. Qu, Z. R. Geng and Z. L. Wang, *J. Mater. Chem. B*, 2012, **22**, 20299–20304.
- 68 Z. Wang, J. Zhang, B. Lu, Y. Li, Y. Liang, J. Yuan, M. Zhao, B. Wang, C. Mai and J. Zhang, *J. Mol. Liq.*, 2019, **296**, 111822.
- 69 X. H. Xia, R. Y. Wan, P. J. Wang, W. R. Huo, H. Dong and Q. Y. Du, *Ecotoxicol. Environ. Saf.*, 2018, **162**, 408–414.
- 70 R. M. Moshikur, M. R. Chowdhury, R. Wakabayashi, Y. Tahara, M. Moniruzzaman and M. Goto, *J. Mol. Liq.*, 2019, **278**, 226–233.
- 71 X. Yang, Q. Y. Chen, X. Li and J. Gao, *Colloids Surf., B*, 2012, **98**, 91–96.
- 72 S. A. Al Sodies, M. R. Aouad, S. Ihmaid, A. Aljuhani, M. Messali, I. Ali and N. Rezki, *J. Mol. Struct.*, 2020, **1207**, 127756.
- 73 K. El Bourakadi, N. Merghoub, G. Hicham, M. E. M. Mekhzoum, E. M. Essassi, A. E. K. Qaiss and R. Bouhfid, *J. Mol. Liq.*, 2019, **282**, 63–69.
- 74 A. N. Duman, I. Ozturk, A. Tuncel, K. Ocakoglu, S. G. Colak, M. Hosgor-Limoncu and F. Yurt, *Heliyon*, 2019, **5**, e02607.
- 75 J. Suchodolski, J. Feder-Kubis and A. Krasowska, *Microbiol. Res.*, 2017, **197**, 56–64.
- 76 E. S. Morais, N. Silva, T. E. Sintra, S. A. O. Santos, B. M. Neves, I. F. Almeida, P. C. Costa, I. Correia-Sa, S. P. M. Ventura, A. J. D. Silvestre, M. G. Freire and C. S. R. Freire, *Carbohydr. Polym.*, 2019, **206**, 187–197.
- 77 Y. Miwa, H. Hamamoto and T. Ishida, *Eur. J. Pharm. Biopharm.*, 2016, **102**, 92–100.
- 78 A. Abednejad, A. Ghaee, E. S. Morais, M. Sharma, B. M. Neves, M. G. Freire, J. Nourmohammadi and A. A. Mehrizi, *Acta Biomater.*, 2019, **100**, 142–157.
- 79 Y. Yu, Z. Y. Yang, S. J. Ren, Y. N. Gao and L. Q. Zheng, *J. Mol. Liq.*, 2020, **299**, 112185.
- 80 J. Niu, G. Tang, J. Tang, J. Yang, Z. Zhou, Y. Gao, X. Chen, Y. Tian, Y. Li, J. Li and Y. Cao, *J. Agric. Food Chem.*, 2021, **69**, 6485–6494.
- 81 K. E. Eckhart, A. M. Arnold, F. A. Starvaggi and S. A. Sydlik, *Biomater. Sci.*, 2021, **9**, 2467–2479.
- 82 Y. Hu, Y. Xing, P. Ye, H. Yu, X. Meng, Y. Song, G. Wang and Y. Diao, *Front. Microbiol.*, 2023, **14**, 1109972.
- 83 X. Chao, C. Zhang, X. Li, H. Lv, G. Ling and P. Zhang, *Biomater. Sci.*, 2022, **10**, 1008–1017.
- 84 T. Gundolf, R. Kalb, P. Rossmanith and P. Mester, *Front. Microbiol.*, 2022, **13**, 883931.
- 85 N. Weyhing-Zerrer, R. Kalb, R. Ossmer, P. Rossmanith and P. Mester, *Ecotoxicol. Environ. Saf.*, 2018, **148**, 467–472.
- 86 J. Liao, X. Yu, Q. Chen, X. Gao, H. Ruan, J. Shen and C. Gao, *J. Membr. Sci.*, 2020, **599**, 117818.
- 87 O. Forero-Doria, C. Parra-Cid, W. Venturini, C. Espinoza, R. Araya-Maturana, F. Valenzuela-Riffo, C. Saldias, A. Leiva, Y. Duarte, J. Echeverria and L. Guzman, *Bioorg. Chem.*, 2022, **126**, 105914.
- 88 M. Wojcieszak, A. Lewandowska, A. Marcinkowska, Ł. Pałkowski, M. Karolak, A. Skrzypczak, A. Syguda and K. Materna, *J. Mol. Liq.*, 2023, **374**, 121300.
- 89 J. Luczak, C. Jungnickel, I. Łacka, S. Stolte and J. Hupka, *Green Chem.*, 2010, **12**, 593–601.
- 90 C. W. Cho, T. P. T. Pham, Y. Zhao, S. Stolte and Y. S. Yun, *Sci. Total Environ.*, 2021, **786**, 147309.
- 91 X. Liu, L. Chang, L. Peng, R. Bai, Y. Wei, C. Ma and H. Liu, *ACS Appl. Mater. Interfaces*, 2021, **13**, 48358–48364.
- 92 L. L. Gu, S. Poddar, Y. J. Lin, Z. H. Long, D. Q. Zhang, Q. P. Zhang, L. Shu, X. Qiu, M. Kam, A. Javey and Z. Y. Fan, *Nature*, 2020, **581**, 278–282.
- 93 W. Florio, S. Becherini, F. D'Andrea, A. Lupetti, C. Chiappe and L. Guazzelli, *Mater. Sci. Eng., C*, 2019, **104**, 109907.
- 94 J. Sommer, S. Fister, T. Gundolf, B. Bromberger, P. J. Mester, A. K. Witte, R. Kalb and P. Rossmanith, *Int. J. Mol. Sci.*, 2018, **19**, 790.
- 95 S. Marullo, G. Gallo, G. Infurna, N. T. Dintcheva and F. D'Anna, *Green Chem.*, 2023, **25**, 3692–3704.
- 96 C. M. Chism, S. Plash, D. Zuckerman, G. S. Dasanayake, M. Bennett, S. K. Tripathi, S. D. Pedigo and E. E. L. Tanner, *ACS Appl. Eng. Mater.*, 2022, **1**, 23–31.
- 97 P. Mester, M. Wagner and P. Rossmanith, *Ecotoxicol. Environ. Saf.*, 2015, **111**, 96–101.
- 98 T. Zhang, B. Sun, J. Guo, M. Wang, H. Cui, H. Mao, B. Wang and F. Yan, *Acta Biomater.*, 2020, **115**, 136–147.
- 99 B. He, Y. Du, B. Wang, X. Wang, Q. Ye and S. Liu, *Prog. Org. Coat.*, 2021, **157**, 106298.
- 100 J. Guo, Q. Xu, Z. Zheng, S. Zhou, H. Mao, B. Wang and F. Yan, *ACS Macro Lett.*, 2015, **4**, 1094–1098.
- 101 L. Guzman, C. Parra-Cid, E. Guerrero-Munoz, C. Penavaras, E. Polo-Cuadrado, Y. Duarte, R. I. Castro, L. S. Nerio, R. Araya-Maturana, T. Asefa, J. Echeverria, D. Ramirez and O. Forero-Doria, *Bioorg. Chem.*, 2021, **115**, 105289.
- 102 B. Bromberger, J. Sommer, C. Robben, C. Trautner, R. Kalb, P. Rossmanith and P.-J. Mester, *Sep. Purif. Technol.*, 2020, **251**, 117309.
- 103 A. Tarannum, R. R. Jonnalagadda and N. F. Nishter, *Spectrochim. Acta, Part A*, 2019, **212**, 343–348.
- 104 T. Clapa, J. Michalski, A. Syguda, D. Narozna, P. van Oostrum and E. Reimhult, *Res. Microbiol.*, 2021, **172**, 103817.
- 105 K. S. Egorova and V. P. Ananikov, *J. Mol. Liq.*, 2018, **272**, 271–300.



- 106 J. Michalski, C. Odrzygóźdź, P. Mester, D. Narożna and T. Cłapa, *J. Mol. Liq.*, 2023, **369**, 120782.
- 107 H. Wang, H. Fan, H. Liu, M. Jin, S. Du, D. Li, P. Zhang, S. Ruan and J. Qiu, *J. Hazard. Mater.*, 2020, **399**, 122847.
- 108 J. Chen, M. Chen, Y. Cheng, C. Fang, J. Luo, X. Zhang and T. Qin, *Carbohydr. Polym.*, 2022, **298**, 120098.
- 109 P. Kowalczyk, A. Borkowski, G. Czerwonka, T. Cłapa, J. Cieśla, A. Misiewicz, M. Borowiec and M. Szala, *J. Mol. Liq.*, 2018, **266**, 540–547.
- 110 J. Suchodolski, J. F. Kubis and A. Krasowska, *J. Biotechnol.*, 2015, **208**, 91.
- 111 G. K. K. Reddy and Y. V. Nancharaiah, *Front. Microbiol.*, 2020, **11**, 730.
- 112 I. C. Ferreira, D. Araujo, P. Voisin, V. D. Alves, A. A. Rosatella, C. A. M. Afonso, F. Freitas and L. A. Neves, *Carbohydr. Polym.*, 2020, **247**, 116679.
- 113 J. L. Shamshina and P. Berton, *Front. Bioeng. Biotechnol.*, 2020, **8**, 11.
- 114 D. O. Hartmann and C. Silva Pereira, *New J. Chem.*, 2013, **37**, 1569–1577.
- 115 M. Petkovic, D. O. Hartmann, G. Adamová, K. R. Seddon, L. P. N. Rebelo and C. S. Pereira, *New J. Chem.*, 2012, **36**, 56–63.
- 116 C. G. Guo and W. K. Leung, *Gut Liver*, 2020, **14**, 179–189.
- 117 N. Klomjit and P. Ungprasert, *Eur. J. Intern. Med.*, 2022, **101**, 21–28.
- 118 Y. Kuwabara, H. Hamamoto, S. Hikake and Y. Miwa, *J. Pain*, 2013, **14**, S73.
- 119 S. N. Riduan and Y. Zhang, *Chem. Soc. Rev.*, 2013, **42**, 9055–9070.
- 120 A. A. Nayl, W. A. A. Arafa, I. M. Ahmed, A. I. Abd-Elhamid, E. M. El-Fakharany, M. A. Abdelgawad, S. M. Gomha, H. M. Ibrahim, A. A. Aly, S. Brase and A. K. Mourad, *Molecules*, 2022, **27**, 2940.
- 121 M. Kuczak, M. Musial, K. Malarz, P. Rurka, E. Zorebski, R. Musiol, M. Dzida and A. Mrozek-Wilczkiewicz, *J. Hazard. Mater.*, 2022, **427**, 128160.
- 122 T. H. Han, J. D. Lee, B. C. Seo, W. H. Jeon, H. A. Yang, S. Kim, K. Haam, M. K. Park, J. Park, T. S. Han and H. S. Ban, *Ecotoxicol. Environ. Saf.*, 2022, **248**, 114334.
- 123 A. Aljuhani, M. R. Aouad, N. Rezki, O. A. Aljaldy, S. A. Al-Sodies, M. Messali and I. Ali, *J. Mol. Liq.*, 2019, **285**, 790–802.
- 124 Z. Deng, C. Fang, X. Ma, X. Li, Y. J. Zeng and X. Peng, *ACS Appl. Mater. Interfaces*, 2020, **12**, 20321–20330.
- 125 C. Ornelas, *New J. Chem.*, 2011, **35**, 1973–1985.
- 126 S. Peter and B. A. Aderibigbe, *Molecules*, 2019, **24**, 3604.
- 127 B. Aneja, N. S. Khan, P. Khan, A. Queen, A. Hussain, M. T. Rehman, M. F. Alajmi, H. R. El-Seedi, S. Ali, M. I. Hassan and M. Abid, *Eur. J. Med. Chem.*, 2019, **163**, 840–852.
- 128 G. Verma, A. Marella, M. Shaquiquzzaman, M. Akhtar, M. R. Ali and M. M. Alam, *J. Pharm. BioAllied Sci.*, 2014, **6**, 69–80.
- 129 S. Pandey, V. K. Sharma, A. Biswas, M. Lahiri and S. Basu, *RSC Med. Chem.*, 2021, **12**, 1604–1611.
- 130 B. Murugesan, M. Arumugam, N. Pandiyan, M. Veerasingam, J. Sonamuthu, S. Samayanan and S. Mahalingam, *Mater. Sci. Eng., C*, 2019, **98**, 1122–1132.
- 131 C. M. Dobson, *Nature*, 2003, **426**, 884–890.
- 132 D. Eisenberg and M. Jucker, *Cell*, 2012, **148**, 1188–1203.
- 133 T. P. J. Knowles, M. Vendruscolo and C. M. Dobson, *Nat. Rev. Mol. Cell Biol.*, 2014, **15**, 384–396.
- 134 A. Basu, S. C. Bhattacharya and G. S. Kumar, *Int. J. Biol. Macromol.*, 2018, **107**, 2643–2649.
- 135 T. Raj, R. Morya, K. Chandrasekhar, D. Kumar, S. Soam, R. Kumar, A. K. Patel and S. H. Kim, *Bioresour. Technol.*, 2023, **369**, 128429.
- 136 Y. Zhao and Y. Zhen, *J. Mol. Liq.*, 2022, **349**, 118185.
- 137 R. M. Moshikur, M. K. Ali, R. Wakabayashi, M. Moniruzzaman and M. Goto, *Mol. Pharmaceutics*, 2021, **18**, 3108–3115.
- 138 G. Jeremias, F. Jesus, S. P. M. Ventura, F. J. M. Goncalves, J. Asselman and J. L. Pereira, *J. Hazard. Mater.*, 2021, **409**, 124517.
- 139 P. Kumari, V. V. S. Pillai and A. Benedetto, *Biophys. Rev.*, 2020, **12**, 1187–1215.
- 140 A. Tarannum, J. R. Rao and N. N. Fathima, *Int. J. Biol. Macromol.*, 2022, **209**, 498–505.
- 141 L. X. Hu, Q. Xiong, W. J. Shi, G. Y. Huang, Y. S. Liu and G. G. Ying, *Ecotoxicol. Environ. Saf.*, 2021, **208**, 111629.
- 142 F. Fadaei, M. Tortora, A. Gessini, C. Masciovecchio, S. Catalini, J. Vigna, I. Mancini, A. Mele, J. Vacek, D. Reha, B. Minofar and B. Rossi, *J. Mol. Liq.*, 2022, **347**, 118350.
- 143 J. Dołzonek, C. W. Cho, P. Stepnowski, M. Markiewicz, J. Thöming and S. Stolte, *Environ. Pollut.*, 2017, **228**, 378–389.
- 144 V. Tsarpali, A. Belavgeni and S. Dailianis, *Aquat. Toxicol.*, 2015, **164**, 72–80.
- 145 J. Liu, Y. Wang, C. Wang, J. Gao, W. Cui, B. Zhao, L. Zhang, H. He and S. Zhang, *J. Phys. Chem. Lett.*, 2021, **12**, 9926–9932.
- 146 M. Galluzzi, L. Marfori, S. Asperti, A. D. Vita, M. Giannangeli, A. Caselli, P. Milani and A. Podesta', *Phys. Chem. Chem. Phys.*, 2022, **24**, 27328.
- 147 L. H. Xiao, H. Y. Guo, B. Cao, G. Mo, Z. H. Li and Z. W. Yu, *Phys. Chem. Chem. Phys.*, 2021, **23**, 17888–17893.
- 148 N. Kaur, M. Fischer, S. Kumar, G. K. Gahlay, H. A. Scheidt and V. S. Mithu, *J. Colloid Interface Sci.*, 2020, **581**, 954–963.
- 149 N. Kaur, S. Kumar, Shiksha, G. K. Gahlay and V. S. Mithu, *J. Phys. Chem. B*, 2021, **125**, 3613–3621.
- 150 M. Kumari, A. Gupta, Shobhna and H. K. Kashyap, *J. Phys. Chem. B*, 2020, **124**, 6748–6762.
- 151 L. Zheng, J. Li, M. Yu, W. Jia, S. Duan, D. Cao, X. Ding, B. Yu, X. Zhang and F. J. Xu, *J. Am. Chem. Soc.*, 2020, **142**, 20257–20269.
- 152 T. M. Abdelghany, A. C. Leitch, I. Nevjestic, I. Ibrahim, S. Miwa, C. Wilson, S. Heutz and M. C. Wright, *Food Chem. Toxicol.*, 2020, **145**, 111593.
- 153 A. Chandran, D. Ghoshdastidar and S. Senapati, *J. Am. Chem. Soc.*, 2012, **134**, 20330–20339.





- 154 S. Sarkar and P. Chandra Singh, *J. Phys. Chem. Lett.*, 2020, **11**, 10150–10156.
- 155 G. Singh, M. Kaur, M. Singh, H. Kaur and T. S. Kang, *Langmuir*, 2021, **37**, 10319–10329.
- 156 A. Pabbathi and A. Samanta, *J. Phys. Chem. B*, 2020, **124**, 8132–8140.
- 157 R. R. Reddy, G. Shanmugam, B. Madhan and B. V. N. Phani Kumar, *Phys. Chem. Chem. Phys.*, 2018, **20**, 9256–9268.
- 158 N. Nikfarjam, M. Ghomi, T. Agarwal, M. Hassanpour, E. Sharifi, D. Khorsandi, M. Ali Khan, F. Rossi, A. Rossetti, E. Nazarzadeh Zare, N. Rabiee, D. Afshar, M. Vosough, T. Kumar Maiti, V. Mattoli, E. Lichtfouse, F. R. Tay and P. Makvandi, *Adv. Funct. Mater.*, 2021, **31**, 2104148.
- 159 W. X. Li, L. Zhu, Z. K. Du, B. Li, J. H. Wang, J. Wang, C. Zhang and L. S. Zhu, *Chemosphere*, 2020, **249**, 126119.
- 160 N. Rezki, F. F. Al-Blewi, S. A. Al-Sodies, A. K. Alnuzha, M. Messali, I. Ali and M. R. Aouad, *ACS Omega*, 2020, **5**, 4807–4815.
- 161 M. Nakano, H. Tateishi-Karimata, S. Tanaka and N. Sugimoto, *J. Phys. Chem. B*, 2014, **118**, 379–389.
- 162 K. Jumbri, M. A. Kassim, N. M. Yunus, M. B. Abdul Rahman, H. Ahmad and R. Abdul Wahab, *Processes*, 2019, **8**, 13.
- 163 H. Y. Wang, J. J. Wang and S. B. Zhang, *Phys. Chem. Chem. Phys.*, 2011, **13**, 3906–3910.
- 164 A. M. O. Azevedo, S. A. P. Pereira, M. L. C. Passos, S. P. F. Costa, P. Pinto, A. Araujo and M. Saraiva, *Chemosphere*, 2017, **173**, 351–358.
- 165 X. Wang, T. Guo, Y. Shu and J. Wang, *Colloids Surf., B*, 2021, **206**, 111971.
- 166 A. Benedetto and P. Ballone, *ACS Sustainable Chem. Eng.*, 2015, **4**, 392–412.
- 167 M. Mukherjee and J. Mondal, *J. Phys. Chem. B*, 2020, **124**, 6565–6574.
- 168 A. A. Khachatrian, T. A. Mukhametzhanov, D. G. Yakhvarov, O. G. Sinyashin, B. F. Garifullin, I. T. Rakipov, D. A. Mironova, V. A. Buriilov and B. N. Solomonov, *J. Mol. Liq.*, 2022, **348**, 118426.
- 169 N. Z. Laird, P. Phruttiwanichakun, M. Zhu, J. A. Banas, S. Elangovan and A. K. Salem, *J. Biomed. Mater. Res.*, 2023, **111**, 682–687.
- 170 X. Wang, T. Guo, Y. Shu and J. Wang, *Colloids Surf., B*, 2021, **206**, 111971.
- 171 G. Singh, M. Kaur, D. Singh, A. K. Kesavan and T. S. Kang, *J. Phys. Chem. B*, 2020, **124**, 3791–3800.
- 172 I. Pacheco-Fernández and V. Pino, Extraction With Ionic Liquids–Organic Compounds, in *Liquid-Phase Extraction, Handbooks in Separation Science*, Elsevier, 2020, pp. 499–537.
- 173 G. Katarzyna and P. Andrzej, *Acta Pol. Pharm.*, 2010, **67**, 3–12.
- 174 A. K. Rössmann, P. Gaertner and K. Bica, *Green Chem.*, 2011, **13**, 1442–1447.
- 175 H. Passos, M. G. Freire and J. A. Coutinho, *Green Chem.*, 2014, **16**, 4786–4815.
- 176 Z. Luo, M. Tian, N. Ahmad, W. Qiu, Y. Zhang, C. Li and C. Zhao, *Colloids Surf., B*, 2023, **222**, 113067.
- 177 S.-C. Zhu, M.-Z. Shi, Y.-L. Yu and J. Cao, *Ind. Crops Prod.*, 2022, **183**, 114968.
- 178 X. Yang, R. Zhao, H. Wang, A. Ben, H. Lin, X. Zhang, C. Li and L. Yang, *Ind. Crops Prod.*, 2022, **187**, 115351.
- 179 R. Wang, Z. Yang, W. Lv, Z. Tan and H. Zhang, *Ind. Crops Prod.*, 2022, **187**, 115465.
- 180 G.-U. Kim, G.-S. Ha, M. B. Kurade, S. Saha, M. A. Khan, Y.-K. Park, W. Chung, S. W. Chang, K. K. Yadav and B.-H. Jeon, *Chem. Eng. J.*, 2022, **446**, 137285.
- 181 B. Gökdemir, N. Baylan and S. Çehreli, *Anal. Lett.*, 2020, **133**, 2111–2121.
- 182 S. Ji, Y. J. Wang, S. K. Gao, X. Shao, W. Cui, Y. Du, M. Z. Guo and D. Q. Tang, *J. Ind. Eng. Chem.*, 2019, **80**, 352–360.
- 183 K. S. Khoo, X. Tan, C. W. Ooi, K. W. Chew, W. H. Leong, Y. H. Chai, S.-H. Ho and P. L. Show, *J. Cleaner Prod.*, 2021, **284**, 124772.
- 184 H. Xu, X. Li, Y. Hao, X. Zhao, Y. Cheng and J. Zhang, *J. Mol. Liq.*, 2021, **333**, 115982.
- 185 G. Shi, L. Lin, Y. Liu, G. Chen, A. Yang, Y. Wu, Y. Zhou and H. Li, *Molecules*, 2021, **26**, 3169.
- 186 X. Sui, T. Liu, J. Liu, J. Zhang, H. Zhang, H. Wang and Y. Yang, *Ultrason. Sonochem.*, 2020, **69**, 105263.
- 187 G. Shi, L. Lin, Y. Liu, G. Chen, S. Fu, Y. Luo, A. Yang, Y. Zhou, Y. Wu and H. Li, *Alexandria Eng. J.*, 2022, **61**, 6897–6906.
- 188 S. Komaty, A. Sauvager, J. P. Bazureau, S. Tomasi and L. Paquin, *Phytochem. Anal.*, 2021, **32**, 592–600.
- 189 P. Chen, X. Liu, L. Wang, C. Wang and J. Fu, *J. Sep. Sci.*, 2021, **44**, 585–599.
- 190 B. Albero, J. L. Tadeo and R. A. Pérez, *TrAC, Trends Anal. Chem.*, 2019, **118**, 739–750.
- 191 N. F. Sukor, R. Jusoh, N. S. Kamarudin, N. A. Abdul Halim, A. Z. Sulaiman and S. B. Abdullah, *Ultrason. Sonochem.*, 2020, **62**, 104876.
- 192 Q. Sun, B. Du, C. Wang, W. Xu, Z. Fu, Y. Yan, S. Li, Z. Wang and H. Zhang, *Chromatographia*, 2019, **82**, 1777–1789.
- 193 C. Q. Li, Y. P. Cui, J. Lu, C. Y. Liu, S. T. Chen, C. Y. Ma, Z. H. Liu, J. M. Wang and W. Y. Kang, *Molecules*, 2020, **25**, 1309.
- 194 R. Rodrigues, P. Lima, R. Santiago-Aguiar and M. Rocha, *Algal Res.*, 2019, **38**, 101391.
- 195 A. Symes, A. Shavandi and A. E. D. A. Bekhit, *Int. J. Food Sci. Technol.*, 2023, **58**, 3935–3945.
- 196 R. F. da Silva, C. N. Carneiro, C. B. D. C. de Sousa, F. J. V. Gomez, M. Espino, J. Boiteux, M. de Los, Á. Fernández, M. F. Silva and F. D. S. Dias, *Microchem. J.*, 2022, **175**, 107184.
- 197 D. Gheidari, M. Mehrdad and S. Maleki, *Appl. Organomet. Chem.*, 2022, **36**, e6631.
- 198 T. M. Dhameliya, P. R. Nagar, K. A. Bhakhar, H. R. Jivani, B. J. Shah, K. M. Patel, V. S. Patel, A. H. Soni, L. P. Joshi and N. D. Gajjar, *J. Mol. Liq.*, 2022, **348**, 118329.
- 199 M. S. Mirakmahaleh, K. Rad-Moghadam, H. Kefayati and S. Falakro, *Mol. Diversity*, 2021, **25**, 109–119.
- 200 N. Wang, Z. Li, Q. Hou, F. Han, Y. Yan, J. Zhang and C. Miao, *J. Org. Chem.*, 2022, **87**, 11669–11680.



- 201 G. Shi, K. Chen, Y. Wang, H. Li and C. Wang, *ACS Sustainable Chem. Eng.*, 2018, **6**, 5760–5765.
- 202 M. A. A. Mohamed, A. M. Kadry, S. A. Bekhit, M. A. S. Abourehab, K. Amagase, T. M. Ibrahim, A. M. M. El-Saghier and A. A. Bekhit, *J. Enzyme Inhib. Med. Chem.*, 2023, **38**, 330–342.
- 203 M. A. Siddiqui, M. H. Shaikh, A. A. Nagargoje, T. T. Shaikh, V. M. Khedkar, P. P. Deshpande and B. B. Shingate, *Res. Chem. Intermed.*, 2022, **48**, 5187–5208.
- 204 H. Ni, Y. Zhang, C. Zong, Z. Hou, H. Song, Y. Chen, X. Liu, T. Xu and Y. Luo, *Int. J. Mol. Sci.*, 2022, **23**, 12877.
- 205 K. Madgula, S. Dandu, S. Kasula and P. Halady, *Inorg. Chem. Commun.*, 2022, **138**, 109218.
- 206 D. D. Chudasama, M. S. Patel, J. N. Parekh, H. C. Patel, C. V. Rajput, N. P. Chikhaliya and K. R. Ram, *Mol. Diversity*, 2023, **27**, 1409–1425.
- 207 M. H. Abdollahi-Basir, B. Mirhosseini-Eshkevari, F. Zamani and M. A. Ghasemzadeh, *Sci. Rep.*, 2021, **11**, 5109.
- 208 P. Patil, A. Yadav, L. Bavkar, N. B. Nippu, N. D. Satyanarayan, A. Mane, A. Gurav, S. Hangirgekar and S. Sankpal, *J. Mol. Struct.*, 2021, **1242**, 130672.
- 209 F. Rezaei, M. Ali Amrollahi and R. Khalifeh, *ChemistrySelect*, 2020, **5**, 1760–1766.
- 210 X. L. Zhu, X. X. Tang, H. Y. Lin, S. G. Shi, H. H. Xiong, Q. J. Zhou, A. Li, Q. Y. Wang, X. Y. Chen and J. H. Gao, *Chem*, 2020, **6**, 1134–1148.
- 211 L. Gao, X. Lin and X. Chen, *Talanta*, 2020, **212**, 120763.
- 212 S. Boobphahom, N. Ruecha, N. Rodthongkum, O. Chailapakul and V. T. Remcho, *Anal. Chim. Acta*, 2019, **1083**, 110–118.
- 213 K. Teekayupak, C. Aumnate, A. Lomae, P. Preechakasedkit, C. S. Henry, O. Chailapakul and N. Ruecha, *Talanta*, 2023, **254**, 124131.
- 214 S. Niyogi, E. Bekyarova, M. E. Itkis, J. L. McWilliams, M. A. Hamon and R. C. Haddon, *J. Am. Chem. Soc.*, 2006, **218**, 7720–7721.
- 215 Y. V. M. Reddy, J. H. Shin, V. N. Palakollu, B. Sravani, C. H. Choi, K. Park, S. K. Kim, G. Madhavi, J. P. Park and N. P. Shetti, *Adv. Colloid Interface Sci.*, 2022, **304**, 102664.
- 216 M. A. Kanjwal and A. A. Ghaferi, *Sensors*, 2022, **22**, 8661.
- 217 H. Zhou, S. Bai, Y. Zhang, D. Xu and M. Wang, *Int. J. Environ. Res. Public Health*, 2022, **19**, 7584.
- 218 H. Yang, C. Shan, F. Li, D. Han, Q. Zhang and L. Niu, *Chem. Commun.*, 2009, 3880–3882.
- 219 D. Wei and A. Ivaska, *Anal. Chim. Acta*, 2008, **607**, 126–135.
- 220 Q. Zhang, W. Cheng, D. Wu, Y. Yang, X. Feng, C. Gao, L. Meng, X. Shen, Y. Zhang and X. Tang, *Food Chem.*, 2022, **367**, 130727.
- 221 F. Luan, S. Zhang, D. D. Chen, F. M. Wei and X. M. Zhuang, *Microchem. J.*, 2018, **143**, 450–456.
- 222 H. Wang, C. Yan, Q. Wu, H. Zeng, Z. Zhang, W. Wang and X. Sun, *J. Orthop. Surg. Res.*, 2023, **18**, 61.
- 223 T. J. Lin, K. T. Yen, C. F. Chen, S. T. Yan, K. W. Su and Y. L. Chiang, *Sensors*, 2022, **22**, 3009.
- 224 Y. Abbas, S. Ali, M. Basharat, W. Zou, F. Yang, W. Liu, S. Zhang, Z. Wu, N. Akhtar and D. Wu, *ACS Appl. Nano Mater.*, 2020, **3**, 11383–11390.
- 225 C. Y. Wang, Y. Y. Wang, H. J. Zhang, H. P. Deng, X. X. Xiong, C. Y. Li and W. W. Li, *Anal. Chim. Acta*, 2019, **1090**, 64–71.
- 226 F. H. Moghadam, M. A. Taher and H. Agheli, *Top. Catal.*, 2022, **65**, 677–683.
- 227 B. Z. Liu, M. Wang and B. Xiao, *J. Electroanal. Chem.*, 2015, **757**, 198–202.
- 228 R. Bavandpour, H. Karimi-Maleh, M. Asif, V. K. Gupta, N. Atar and M. Abbasghorbani, *J. Mol. Liq.*, 2016, **213**, 369–373.
- 229 U. Nishan, F. Bashir, N. Muhammad, N. Khan, A. Rahim, M. Shah, R. Nazir and M. Sayed, *J. Mol. Liq.*, 2019, **294**, 111681.
- 230 K. Kunpatee, S. Traipop, O. Chailapakul and S. Chuanuwatanakul, *Sens. Actuators, B*, 2020, **314**, 128059.
- 231 H. Liu, R. Jamal, T. Abdiryim, R. Simayi, L. Liu and Y. Liu, *ACS Sustainable Chem. Eng.*, 2021, **9**, 5860–5871.
- 232 L. Farzin, S. Sadjadi, M. Shamsipur and S. Sheibani, *J. Pharm. Biomed. Anal.*, 2020, **179**, 112989.
- 233 X. Wang, L. Shang, W. Zhang, L. P. Jia, R. N. Ma, W. L. Jia and H. S. Wang, *Biosens. Bioelectron.*, 2019, **141**, 111436.
- 234 M. Roostaei, H. Beitollahi and I. Sheikhsheoae, *Micromachines*, 2022, **13**, 1834.
- 235 Q. W. Peng, X. Y. Yan, X. R. Shi, S. S. Ou, H. Gu, X. X. Yin, G. Y. Shi and Y. Y. Yu, *Biosens. Bioelectron.*, 2019, **144**, 111665.
- 236 G. Vilagut, C. G. Forero, A. Pinto-Meza, J. M. Haro, R. de Graaf, R. Bruffaerts, V. Kovess, G. de Girolamo, H. Matschinger, M. Ferrer and J. Alonso, *Value Health*, 2013, **16**, 564–573.
- 237 M. W. Petersen, E. Ornbol, T. M. Dantoft and P. Fink, *J. Psychosom. Res.*, 2021, **146**, 110491.
- 238 R. Koirala, E. G. Iyer Soegaard, Z. Kan, S. P. Ojha, E. Hauff and S. B. Thapa, *J. Psychiatr. Res.*, 2021, **143**, 23–29.
- 239 E. Nagles, O. Garcia-Beltrán and J. A. Calderón, *Electrochim. Acta*, 2017, **258**, 512–523.
- 240 Y. H. Li, Y. Ji, B. B. Ren, L. N. Jia, G. D. Ma and X. S. Liu, *Mater. Res. Bull.*, 2019, **109**, 240–245.
- 241 S. Yang, W. Feng, L. Xue, M. Yin, B. Li, L. Lu, F. Dai, J. Jiao and Q. Chen, *Biosens. Bioelectron.*, 2022, **201**, 113972.
- 242 E. L. Grafe, C. J. Fontaine, J. D. Thomas and B. R. Christie, *J. Neurophysiol.*, 2021, **126**, 1622–1634.
- 243 A. Llorente-Ovejero, J. Martinez-Gardeazabal, M. Moreno-Rodriguez, L. Lombardero, E. Gonzalez de San Roman, I. Manuel, M. T. Giralt and R. Rodriguez-Puertas, *ACS Chem. Neurosci.*, 2021, **12**, 2167–2181.
- 244 D. A. El Hady and A. K. Youssef, *Anal. Chim. Acta*, 2013, **772**, 68–74.
- 245 D. A. El Hady, H. M. Albishri and H. Watzig, *Electrophoresis*, 2016, **37**, 1609–1623.
- 246 M. I. Holubiec, M. Gellert and E. M. Hanschmann, *Front. Aging Neurosci.*, 2022, **14**, 1003721.
- 247 Z. R. Lou, P. Li and K. L. Han, *Acc. Chem. Res.*, 2015, **48**, 1358–1368.
- 248 Y. Yang, L. Wang, H. Q. Cao, Q. Li, Y. Li, M. J. Han, H. Wang and J. B. Li, *Nano Lett.*, 2019, **19**, 1821–1826.



- 249 W. Wu, C. Zhang, T. W. Rees, X. Liao, X. Yan, Y. Chen, L. Ji and H. Chao, *Anal. Chem.*, 2020, **92**, 6003–6009.
- 250 W. Gao, Y. Zhang, Y. Zheng, H. Zhang, X. Wang, L. Bai, Y. Wu and X. Ba, *J. Nanopart. Res.*, 2020, **22**, 342.
- 251 L. F. Gao, X. L. Lin, A. Q. Zheng, E. Shuang, J. H. Wang and X. W. Chen, *Anal. Chim. Acta*, 2020, **1111**, 132–138.
- 252 P. Lesani, G. Singh, Z. Lu, M. Mirkhalaf, E. J. New and H. Zreiqat, *Chem. Eng. J.*, 2022, **433**, 133668.
- 253 A. Steinegger, O. S. Wolfbeis and S. M. Borisov, *Chem. Rev.*, 2020, **120**, 12357–12489.
- 254 X. Ye, Y. Xiang, Q. Wang, Z. Li and Z. Liu, *Small*, 2019, **15**, e1901673.
- 255 B. A. Webb, M. Chimenti, M. P. Jacobson and D. L. Barber, *Nat. Rev. Cancer*, 2011, **11**, 671–677.
- 256 X. Yu, X. Yuan, Z. Huang, W. Zhang, F. Huang and L. Ren, *ACS Biomater. Sci. Eng.*, 2020, **6**, 6405–6414.
- 257 G. B. Yang, L. G. Xu, J. Xu, R. Zhang, G. S. Song, Y. Chao, L. Z. Feng, F. X. Han, Z. L. Dong, B. Li and Z. Liu, *Nano Lett.*, 2018, **18**, 2475–2484.
- 258 M. Amaral, A. B. Pereira, M. M. Gaspar and C. P. Reis, *Nanomedicine*, 2021, **16**, 63–80.
- 259 W.-X. Zhang, Y.-R. Gao, R. Xue, W. Nguyen, W. Chen, J.-H. Wang and Y. Shu, *Mater. Today Phys.*, 2023, **30**, 100925.
- 260 D. A. S. Agostinho, A. R. Jesus, A. B. P. Silva, J. Esperanca, A. Paiva, A. R. C. Duarte and P. M. Reis, *J. Pharm. Sci.*, 2021, **110**, 2489–2500.
- 261 J. Yuan, N. Zhou, J. Wu, T. Yin and Y. Jia, *RSC Adv.*, 2022, **12**, 3416–3422.
- 262 Y. Shi, Z. Zhao, Y. Gao, D. C. Pan, A. K. Salinas, E. E. L. Tanner, J. Guo and S. Mitragotri, *J. Controlled Release*, 2020, **322**, 602–609.
- 263 B. Lu, M. Yi, S. Hu, D. Wu, Z. Zhu, C. Wu, Z. Wang, Y. Li and J. Zhang, *ACS Sustainable Chem. Eng.*, 2021, **9**, 5991–6000.
- 264 L. Shen, Y. Zhang, J. Feng, W. Xu, Y. Chen, K. Li, X. Yang, Y. Zhao, S. Ge and J. Li, *ACS Appl. Mater. Interfaces*, 2022, **14**, 45229–45239.
- 265 C. Agatemor, K. N. Ibsen, E. E. L. Tanner and S. Mitragotri, *Bioeng. Transl. Med.*, 2018, **3**, 7–25.
- 266 Y. Tahara, K. Morita, R. Wakabayashi, N. Kamiya and M. Goto, *Mol. Pharmaceutics*, 2020, **17**, 3845–3856.
- 267 M. Zakrewsky and S. Mitragotri, *J. Controlled Release*, 2016, **242**, 80–88.
- 268 I. J. Lee, Y. H. Lan, P. Y. Wu, Y. W. Wu, Y. H. Chen, S. C. Tseng, T. J. Kuo, C. P. Sun, J. T. Jan, H. H. Ma, C. C. Liao, J. J. Liang, H. Y. Ko, C. S. Chang, W. C. Liu, Y. A. Ko, Y. H. Chen, Z. L. Sie, S. I. Tsung, Y. L. Lin, I. H. Wang and M. H. Tao, *Emerging Microbes Infect.*, 2023, **12**, 2149353.
- 269 S. Saha, A. Sannigrahi, K. Chattopadhyay and J. Chowdhury, *J. Mol. Liq.*, 2020, **301**, 112475.
- 270 J. Huang, M. Wang, F. Zhang, S. Shao, Z. Yao, X. Zhao, Q. Hu and T. Liang, *Adv. Sci.*, 2023, **10**, e2206756.
- 271 A. Ukidve, K. Cu, M. Goetz, P. Angsantikul, A. Curreri, E. E. L. Tanner, J. Lahann and S. Mitragotri, *Adv. Mater.*, 2020, **32**, e2002990.
- 272 X. Lin, Y. Sheng, X. Zhang, Z. Li, Y. Yang, J. Wu, Z. Su, G. Ma and S. Zhang, *J. Controlled Release*, 2022, **346**, 380–391.
- 273 B. Ou, Y. Yang, H. Lv, X. Lin and M. Zhang, *BioDrugs*, 2023, **37**, 143–180.
- 274 L. H. Su, Q. Wu, L. F. Tan, Z. B. Huang, C. H. Fu, X. L. Ren, N. Xia, Z. Z. Chen, X. Y. Ma, X. D. Lan, Q. Zhang and X. W. Meng, *ACS Appl. Mater. Interfaces*, 2019, **11**, 10520–10531.
- 275 X. W. Chen, C. H. Fu, Y. Q. Wang, Q. R. Wu, X. W. Meng and K. Xu, *Nanoscale*, 2018, **10**, 15677–15685.
- 276 Q. Wu, N. Xia, D. Long, L. F. Tan, W. Rao, J. Yu, C. H. Fu, X. L. Ren, H. B. Li, L. Gou, P. Liang, J. Ren, L. F. Li and X. W. Meng, *Nano Lett.*, 2019, **19**, 5277–5286.
- 277 D. K. Pandey, M. Kuddushi, A. Kumar and D. K. Singh, *Colloids Surf., A*, 2022, **650**, 129631.
- 278 J. Zhou, J. Zhang, Y. Sun, F. Luo, M. Guan, H. Ma, X. Dong and J. Feng, *Int. J. Biol. Macromol.*, 2023, **244**, 125263.
- 279 Z. Zhou, Y. Gao, G. Tang, Y. Tian, Y. Li, H. Wang, X. Li, X. Yu, Z. Zhang, Y. Li, Y. Liu and Y. Cao, *Chem. Eng. J.*, 2022, **446**, 137073.
- 280 Y. Yu, Q. Wu, M. Niu, L. Gou, L. Tan, C. Fu, X. Ren, J. Ren, Y. Zheng and X. Meng, *Biomater. Sci.*, 2022, **10**, 3503–3513.
- 281 W. Cui, X. M. Lu, K. Cui, L. Y. Niu, Y. Wei and Q. H. Lu, *Langmuir*, 2012, **28**, 9413–9420.
- 282 B. B. Lu, G. X. Zhou, F. Xiao, Q. J. He and J. H. Zhang, *J. Mater. Chem. B*, 2020, **8**, 7994–8001.
- 283 H. Albadawi, Z. Zhang, I. Altun, J. Hu, L. Jamal, K. N. Ibsen, E. E. L. Tanner, S. Mitragotri and R. Oklu, *Sci. Transl. Med.*, 2021, **13**, eabe3889.
- 284 T. A. Shmool, A. P. Constantinou, A. Jirkas, C. Zhao, T. K. Georgiou and J. P. Hallett, *Polym. Chem.*, 2022, **13**, 2340–2350.
- 285 Y. Shu, R. Xue, Y. Gao, W. Zhang and J. Wang, *J. Mater. Chem. B*, 2023, **11**, 5494–5502.
- 286 X. Qu, J. Liu, S. Wang, J. Shao, Q. Wang, W. Wang, L. Gan, L. Zhong, X. Dong and Y. Zhao, *Chem. Eng. J.*, 2023, **453**, 139785.
- 287 C. Mukesh, J. Bhatt and K. Prasad, *Macromol. Chem. Phys.*, 2014, **215**, 1498–1504.
- 288 C. M. Hamadani, M. J. Goetz, S. Mitragotri and E. E. L. Tanner, *Sci. Adv.*, 2020, **6**, eabd7563.
- 289 P. Khare, S. X. Edgecomb, C. M. Hamadani, E. E. L. Tanner and D. S. Manickam, *Adv. Drug Delivery Rev.*, 2023, **197**, 114861.
- 290 C. M. Hamadani, G. S. Dasanayake, M. E. Gorniak, M. C. Pride, W. Monroe, C. M. Chism, R. Heintz, E. Jarrett, G. Singh, S. X. Edgecomb and E. E. L. Tanner, *Nat. Protoc.*, 2023, **18**, 2509–2557.

